Journal of Paleontology

www.cambridge.org/jpa

Articles

Cite this article: Datta D., and Bajpai S. 2025. Fossil snakes from the Eocene of India: new material with comments on phylogenetic relations and biogeographic and paleoecological implications. *Journal of Paleontology*, 1–27
https://doi.org/10.1017/jpa.2025.10101

Received: 02 July 2024
Revised: 04 January 2025
Accepted: 09 January 2025

Corresponding authors:
Debajit Datta and Sunil Bajpai;
Emails: debajitdatta9@gmail.com; sunil.bajpai@es.iitr.ac.in;
debajitdatta.pd@es.iitr.ac.in

Handling Editor:
Hans-Dieter Sues

JOURNAL OF PALEONTOLOGY
A PUBLICATION OF THE Paleontological SOCIETY

CAMBRIDGE UNIVERSITY PRESS

Fossil snakes from the Eocene of India: new material with comments on phylogenetic relations and biogeographic and paleoecological implications

Debajit Datta and Sunil Bajpai

Department of Earth Sciences, Indian Institute of Technology Roorkee, Roorkee, Uttarakhand 247667, India

Abstract

Eocene snakes of India have the potential to shed light on the nature of snake diversification on the subcontinent following the Deccan volcanism at the Cretaceous-Paleogene boundary (K-Pg), when India was still a northward-drifting isolated landmass prior to its collision with Asia. Here, we report a diverse snake fauna from the Eocene of Kutch, western India. The fauna, dominated by aquatic forms, includes palaeophiids, a giant madtsoiid, and a possible nigerophiid. The palaeophiids from the middle Eocene (late Lutetian) comprise ?*Palaeophis* Owen, 1841 and *Pterosphenus rannensis* n. sp. Together, these taxa enrich the record of fossil snakes in the poorly known late Lutetian of India and represent the youngest record of Palaeophiidae from the Indian subcontinent. *Pterosphenus rannensis* n. sp. shows intermediate morphology between *Palaeophis* and *Pterosphenus*-grade snakes and is phylogenetically the earliest-diverging member of *Pterosphenus* Lucas, 1898. Additionally, the middle Eocene *Pterosphenus biswasi* Rage et al., 2003 is reassessed and retained as a valid taxon based on pterapophyseal morphology and overall form. Biogeographic considerations highlight the importance of the Indian fossil record in understanding the origin and diversification of the genus *Pterosphenus.* The prevalence of niche partitioning is suggested for the palaeophiids, with *Pterosphenus rannensis* n. sp. recovered from a tidal setting and ?*Palaeophis* sp. indet. from a marsh/swamp setting. The new Indian madtsoiid from the middle Eocene (early Lutetian) represents a sympatric taxon with the terrestrial/semiaquatic giant *Vasuki indicus* Datta and Bajpai, 2024 coexisting in a back-swamp marsh setting. The early Eocene (Ypresian) nigerophiid is among the oldest Cenozoic occurrences of this family globally.

UUID: http://zoobank.org/dc529074-73a6-4869-9b49-44caf9e2d956

Non-technical Summary

The Indian Eocene snake fauna is of great importance for understanding the nature of snake diversification on the Indian subcontinent after the Cretaceous-Palaeogene boundary (K-Pg) approximately 66 million years ago. This boundary represents a dramatic time interval in India's geological history because it witnessed one of the most extensive episodes of volcanic activity—the Deccan Traps volcanism. The Indian subcontinent was still drifting northward during this interval before colliding with Asia. Here, we describe a diverse snake fauna from early and middle Eocene of India (between 42 and 56 million years before present), comprising both aquatic (palaeophiid and nigerophiid) and giant terrestrial/semiaquatic (madtsoiid) snakes. The palaeophiids include *Pterosphenus rannensis* n. sp. and represent the geologically youngest record of the family Palaeophiidae from the subcontinent. Additionally, a previously described middle Eocene species, *Pterosphenus biswasi*, is reexamined here and retained as a valid taxon. The palaeophiid snakes described here suggest a considerable diversity of habitats occupied by these fossil snakes. The new finds also highlight the importance of the Indian fossil record in understanding the origin and diversification of the genus *Pterosphenus.* The madtsoiid snake described here lived alongside the recently described gigantic madtsoiid snake *Vasuki indicus.* The nigerophiid snake described here is among the oldest known post-K-Pg extinction record of the family Nigerophiidae globally.

Introduction

The Eocene strata in the Gujarat state of western India preserve a rich diversity of fossil snakes (Rage et al., 2003, 2008; Bajpai and Head, 2007; Smith et al., 2016; Smith and Georgalis, 2022; Datta and Bajpai, 2024). When seen in conjunction with the Late Cretaceous record (Wilson

Mantilla et al., 2010; Rage et al., 2020), the Paleogene snake fauna has the potential to provide significant insights into the biotic effect of India's geographic isolation during its northward drift and its subsequent collision with Asia (Chatterjee et al., 2017). The influence on contemporary biota is especially significant from the perspectives of: (1) possible endemism during India's physical isolation and its evolving faunal affinities from essentially Gondwanan to cosmopolitan as a result of the Indian-Asia collision, and (2) the nature of faunal diversification and turnover across the interval of Deccan volcanic activity at the Cretaceous-Paleogene (K-Pg) boundary.

In India, fossil snakes predating the K-Pg mass extinction are exclusively Maastrichtian in age and known from the terrestrial Lameta Formation and intertrappean beds associated with the Deccan Trap volcanics (Jain and Sahni, 1983; Gayet et al., 1984; Prasad and Sahni, 1987; Rage and Prasad, 1992; Prasad and Rage, 1995; Rage et al., 2004, 2020; Head et al., 2022). This fauna is represented by both stem snakes (*Coniophis* sp., *Sanajeh indicus* Wilson Mantilla et al., 2010; Rage et al., 2004; Wilson Mantilla et al., 2010; Zaher et al., 2023) and members of the crown group Serpentes, e.g., madtsoiids (e.g., *Madtsoia pisdurensis* Mohabey et al., 2011) and nigerophiids (*Indophis sahnii* Rage and Prasad, 1992; Rage et al., 2004, 2020). The post-K-Pg fauna in India is characterized by the appearance of palaeophiids—e.g., *Palaeophis vastaniensis* (Bajpai and Head, 2007); *Pterosphenus kutchensis* Rage et al., 2003; *Pterosphenus schucherti* Lucas, 1898 (Rage et al., 2003; Bajpai and Head, 2007; Natarajan et al., 2024)—constrictors (Rage et al., 2008; see Pyron et al., 2014; Georgalis and Smith, 2020), and caenophidians (colubroideans and *Thaumastophis* Rage et al., 2008; Zaher et al., 2021), along with holdovers from the Cretaceous (madtsoiids, e.g., *Platyspondylophis* Smith et al., 2016 and *Vasuki* Datta and Bajpai, 2024). These taxa are almost exclusively from the early Eocene (Ypresian) Cambay Shale Formation and from the early middle Eocene (Lutetian) horizons of the Naredi Formation (Rage et al., 2003, 2008; Datta and Bajapi, 2024). Conversely, fossil records from the Paleocene and the later parts of the Eocene are poor or nonexistent and include the recently described *Pterosphenus schucherti* from the Harudi Formation that constitutes the sole record from the late middle Eocene of India. Younger records include those from the late Oligocene of Ladakh molasse (e.g., Wasir et al., 2021).

The present study describes new material collected from the early and middle Eocene of Kutch (= Kachchh), Gujarat, western India. This discovery provides new insights into the diversity and phylogenetic relationships of the Indian Eocene snakes. The taxa described in this study significantly improve our understanding of the diversity and pattern of faunal turnover across the K-Pg boundary in India.

Geological setting

The Kutch Basin is a pericratonic rift basin situated along the western continental margin of India and includes one of the most well-preserved marine Tertiary sequences on the subcontinent (Biswas, 1992; Catuneanu and Dave, 2017). These Tertiary sequences are exposed as crescentic belts in the southwestern region of the Kutch mainland along the periphery of the Mesozoic highs. The Paleogene succession of Kutch includes the Matanomadh, Naredi, Harudi, Fulra limestone, and Maniyara Fort formations, in successive order (Biswas, 1992). The present study deals with fossil snakes recovered from the Naredi and Harudi formations (Fig. 1).

Within the Naredi Formation, fossils were collected from the type section and the lignite-bearing Panandhro area of western Kutch. The type section (23°34.602'N, 68°38.628'E), exposed in the cliffs along the Kakdi River, rests unconformably on weathered basalts of the Deccan Traps (Biswas, 1992). It includes three members, the basalmost of which is a gypsiferous Shale Member comprising glauconitic shale and claystone, succeeded by a Ferruginous Claystone Member, and the *Assilina*-bearing Limestone Member on top. The snake-yielding horizon in the type section of the Naredi Formation consists of grayish green silty clays and is located 2 m above the base of the section. This horizon is Ypresian in age and ~1 m below the interval dated as SBZ8 corresponding to planktic foraminiferal zone P6 (= E3—E4; Serra-Kiel et al., 1998; Keller et al., 2013). Based on small benthic and rare planktic foraminiferans, a normal marine inner-shelf environment was suggested for this horizon (Keller et al., 2013).

Elsewhere, the snake-yielding unit in the lignite-bearing succession of the Panandhro area of Kutch (23°41.897'N, 68°46.531'E) lies above the top lignite seam. Besides snakes (*Pterosphenus* Lucas, 1898; Madtsoiidae/Boidae), this unit previously produced a diverse array of taxa including rays and sharks (*Myliobatis* Cuvier, 1816; *Galeocerdo* Müller and Henle, 1837), bony fishes (e.g., the catfish *Arius* Cuvier and Valenciennes, 1840), crocodilians, and archaic whales (*Andrewsiphius* Sahni and Mishra, 1975; *Kutchicetus* Bajpai and Thewissen, 2000) (Bajpai and Thewissen, 2002; Rage et al., 2003). Initially this unit was thought to be early Eocene (Ypresian) in age following Biswas (1992), but more recent investigations proposed an early middle Eocene (early Lutetian) age for the snake-bearing strata above the topmost lignite seam based on age-diagnostic palynomorphs and dinoflagellate cysts (Agrawal et al., 2017), a proposal which was followed later by Datta and Bajpai (2024). A back-swamp environment has been suggested for this unit and the lignite succession (Mukhopadhyay and Shome, 1996; Agrawal et al., 2017).

The Harudi Formation is a shale-dominated unit bearing yellow limonitic partings in the lower part and calcareous claystone and siltstone in the upper part (Biswas, 1992). Snake fossils were recovered from horizons exposed at Godhatad (23°39.1'N, 68°45.2'E), Dhedidi North (23°46'42"N, 68°47'16"E), and Babia Hill (23°41'N, 68°45.4'E) localities that are also known to yield a host of archaic whales (protocetids, remingtonocetids, andrewsiphiines, and remingtonocetines) and sirenians (Bajpai et al., 2006; Thewissen and Bajpai, 2009). A late Lutetian age was assigned to the whale-bearing horizons of the Harudi Formation based on $^{87}Sr/^{86}Sr$ values (Ravikant and Bajpai, 2010). The depositional setting of the snake-yielding localities at Godhatad and Babia Hill were interpreted to represent tidal and swampy/marshy environments, respectively (Mukhopadhyay and Shome, 1996; Thewissen and Bajpai, 2009).

Material and methods

Material. A total of 14 vertebrae from the five fossil localities (see Geological setting) were studied, the details of which are given in Appendix 1. All specimens are housed in the Vertebrate Paleontology Laboratory of the Department Earth Sciences, Indian Institute of Technology Roorkee. For comparative purposes the following taxa/families were studied: Palaeophiidae—*Palaeophis vastaniensis* Bajpai and Head, 2007; *Palaeophis maghrebianus* Arambourg, 1952 (see Houssaye et al., 2013); *Palaeophis africanus* Andrews, 1924 (see Parmley and DeVore, 2005; Folie et al., 2021; Georgalis et al., 2021a); *Palaeophis casei* Holman, 1982; *Palaeophis*

https://doi.org/10.1017/jpa.2025.10101 Published online by Cambridge University Press

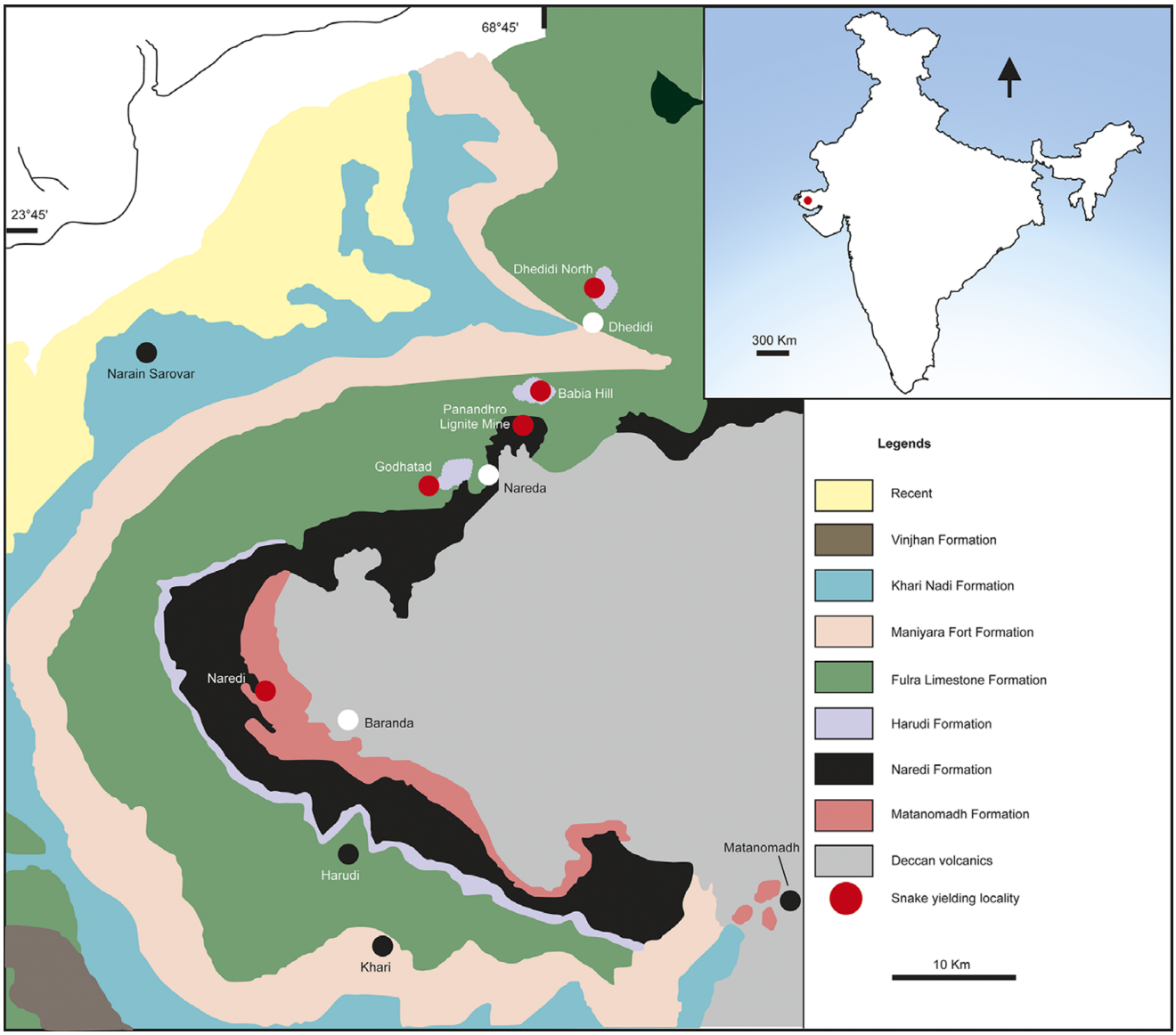

Figure 1. Geological map of Kutch Basin (after Biswas, 1992) showing snake fossil yielding localities. Light purple patches represent discontinuous outcrops of the Harudi Formation.

oweni Zigno, 1881 (see Georgalis et al., 2020); *Palaeophis typhaeus* Owen, 1850 (see Rage, 1983a); *Palaeophis colossaeus* Rage, 1983a (see McCartney et al., 2018; Georgalis et al., 2021a); *Palaeophis nessovi* Averianov, 1997 (see Snetkov, 2011); *Palaeophis toliapicus* Owen, 1841 (see Owen, 1850; Rage, 1983b; Zvonok and Snetkov, 2012); *Pterosphenus schucherti* Lucas, 1898 (see Calvert et al., 2022; Natarajan et al., 2024); *Pterosphenus schweinfurthi* Andrews, 1901 (see McCartney and Seiffert, 2016; Georgalis, 2023); *Pterosphenus sheppardi* Hoffstetter, 1958; *Pterosphenus muruntau* Averianov, 1997 (Averianov, 2023); *Pterosphenus kutchensis* Rage et al., 2003; *Pterosphenus biswasi* Rage et al., 2003; *Archaeophis proavus* Janensch, 1906; and '*Archaeophis*' *turkmenicus* Tatarinov, 1963 (Tatarinov, 1963; Rage, 1984; Rage et al., 2003); Madtsoiidae—*Platyspondylophis tadkeshwarensis* Smith et al., 2016 (Smith et al., 2016); and *Vasuki indicus* Datta and Bajpai, 2024; and Nigerophiidae—*Nigerophis mirus* Rage, 1975; *Kelyophis hechti* LaDuke et al., 2010; *Indophis fanambinana* Pritchard et al., 2014; and *Indophis sahnii* (see Rage, 1975; Rage and Prasad, 1992; LaDuke et al., 2010; Pritchard et al., 2014).

Methods. The osteological description of the vertebrae follows the terminology of Rage (1984), Rage et al. (2003), LaDuke et al. (2010), Rio and Mannion (2017), and Szyndlar and Georgalis (2023). Different parameters (following Datta and Bajpai, 2024; Natarajan et al., 2024) of the specimens were measured (Fig. 2) using Mitutoyo digital callipers with a precision of 0.01 mm and explanatory line drawings have been used where necessary. The terminology of the vaulting ratio of the neural arch (VR) follows Georgalis et al. (2021b). The holotype and referred specimens of *Pterosphenus kutchensis*, *Pterosphenus biswasi*, and *Vasuki indicus* were studied first-hand for comparative and phylogenetic analysis. Published literature and photographs were referred for information on other ophidian taxa.

Abbreviations for measured parameters. CL, centrum length; CNH, condyle height; CNW, condyle width; COH, cotyle height; COW,

https://doi.org/10.1017/jpa.2025.10101 Published online by Cambridge University Press

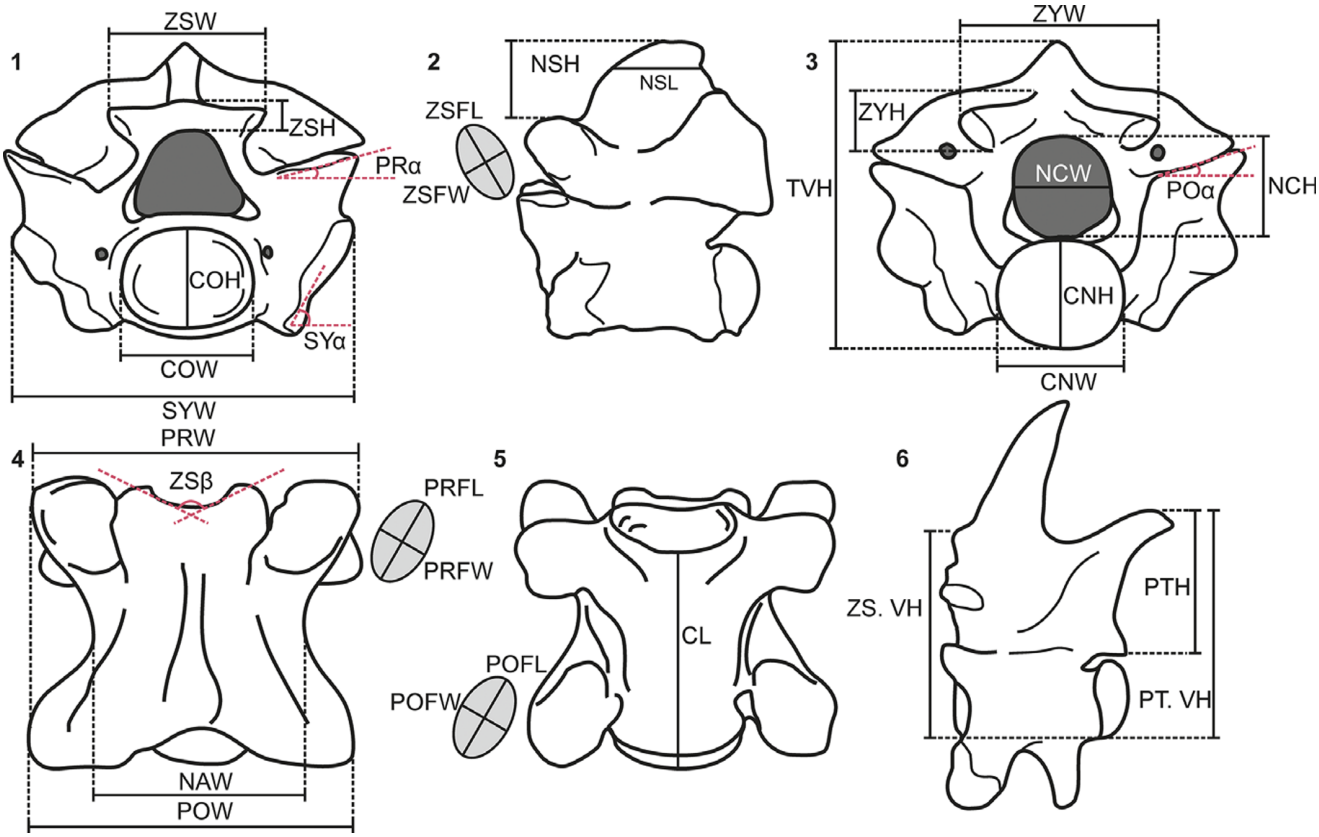

Figure 2. Measured parameters on schematic diagrams: (**1–5**) basic snake vertebra, (**6**) generalized *Pterosphenus* vertebra: (**1**) anterior, (**2, 6**) lateral, (**3**) posterior, (**4**) dorsal, and (**5**) ventral views. Vertebral measurements follow Datta and Bajpai (2024) and Natarajan et al. (2024). CL = centrum length; CNH = condyle height; CNW = condyle width; COH = cotyle height; COW = cotyle width; NAW = neural arch width; NCH = neural canal height; NCW = neural canal width; NSH = neural spine height; NSL = neural spine width; POFL = postzygapophyseal facet length; POFW = postzygapophyseal facet width; POW = postzygapophyseal width; POα = postzygapohyseal angle; PRFL = prezygapophyseal facet length; PRFW = prezygapophyseal facet width; PRW = prezygapophyseal width; PRα = prezygapophyseal angle; PTH = height of pterapophysis; PT.VH = vertebral height from base of condyle to dorsal tip of pterapophysis; SYα = synapophyseal angle; SYW = synapophyseal width; TVH = total vertebral height; ZS.VH = vertebral height from base of condyle to dorsal tip of zygosphene; ZSFL = zygosphenal facet length; ZSFW = zygosphenal facet width; ZSH = zygosphene height; ZSW = zygosphene width; ZSβ = zygosphene angle; ZYH, height of zygantrum; ZYW, width of zygantrum. Schematic diagrams not to scale and after Datta and Bajpai (2024) (**1–5**), Rage et al. (2003) and Garberoglio et al. (2024) (**6**).

cotyle width; NAW, neural arch width; NCH, neural canal height; NCW, neural canal width; NSH, neural spine height; NSL, neural spine length; POFL, postzygapophyseal facet length; POFW, postzygapophyseal facet width; POW, postzygapophyseal width; POα, postzygapohyseal angle; PRFL, prezygapophyseal facet length; PRFW, prezygapophyseal facet width; PRW, prezygapophyseal width; PRα, prezygapophyseal angle; PTH, height of pterapophysis; PT.VH, vertebral height from base of condyle to dorsal tip of pterapophysis; SYα, synapophyseal angle; SYW, synapophyseal width; TVH, total vertebral height; VR, vaulting ratio; ZS.VH, vertebral height from base of condyle to dorsal tip of zygosphene; ZSFL, zygosphenal facet length; ZSFW, zygosphenal facet width; ZSH, zygosphene height; ZSW, zygosphene width; ZSβ, zygosphene angle; ZYH, height of zygantrum; ZYW, width of zygantrum.

Other abbreviations. ATV, anterior trunk vertebrae; MTV, middle trunk vertebrae; PTV, posterior trunk vertebrae; TV, trunk vertebrae.

Repository and institutional abbreviations. CGM, Egyptian Geological Museum, Cairo, Egypt; DPC, Duke Lemur Center, Durham, North Carolina, USA; GCVP, Georgia College Vertebrate Paleontology Collection, Georgia, USA; GU/RSR/VAS, Department of Geology, H.N.B. Garhwal University, Uttaranchal, India; IITBR1, Indian Institute of Technology Bombay, Mumbai, Maharashtra, India; IITR/VPL/SB, Vertebrate Paleontology Laboratory, Indian Institute of Technology Roorkee, Roorkee, India; MGP-PD, Museo di Geologia e Paleontologia dell'Università di Padova, Italy; MNHN, Muséum National d'Histoire Naturelle, Paris, France; MSUVP, Michigan State University Museum, East Lansing; NHMUK, The Natural History Museum, London, UK; NHMW, Naturhistorisches Museum Wien, Vienna, Austria; OCP, Office Chérifien des Phosphates, Khouribga, Morocco; PU, Museum of Natural History of Princeton University, Princeton, New Jersey; RMCA-RGP, Royal Museum for Central Africa—Registre Général Paléontologie, Tervuren, Belgium; RUSB, Roorkee University/Sunil Bajpai/Vertebrate Paleontology Laboratory; USNM, National Museum of Natural History (= United States National Museum), Washington, D.C.; VPL/JU, Vertebrate Paleontology Laboratory, University of Jammu; ZIN PC, Paleontological collection, Zoological Institute, Russian Academy of Sciences, Saint Petersburg, Russia; ZIN PH, Paleoherpetological collection, Zoological Institute, Russian Academy of Sciences, Saint Petersburg, Russia.

Systematic paleontology

Squamata Oppel, 1811
Order **Serpentes** Linnaeus, 1758
Family **Palaeophiidae** Lydekker, 1888
Subfamily **Palaeophiinae** Lydekker, 1888
Genus ***Pterosphenus*** Lucas, 1898

https://doi.org/10.1017/jpa.2025.10101 Published online by Cambridge University Press

Type species. *Pterosphenus schucherti* Lucas, 1898 from the late Lutetian or early Bartonian, and Priabonian, USA.

Pterosphenus rannensis new species
Figures 3–6

Holotype. A partial vertebral column comprising 11 vertebrae (IITR/VPL/SB 3014-1–10, 3015) pertaining to the precloacal region (Appendix 1) from Godhatad, district Kutch, Gujarat state, western India.

Differential diagnosis. *Pterosphenus rannensis* n. sp. is assigned to Palaeophiinae based on the following combination of characters: presence of pterapophyses, posterior hypapophysis in anterior and middle trunk vertebrae, anterior hypapophysis in ATV, extension of synapophyses ventral to the centrum. The following combination of characters further designates this snake to *Pterosphenus*: triangular zygosphene in anterior view, neural spine originating from the anterior margin of the zygosphenal roof, weakly inclined prezygapophyseal facets. Additionally, *Pterosphenus rannensis* n. sp. is diagnosed based on a unique combination of following characters: differs from all other *Pterosphenus* species in ventral positioning of the pterapophysis relative to the dorsal roof of the zygosphene and shallow ventral extension of the synapophyses in MTV; differs from *Pterosphenus kutchensis* and *Pterosphenus biswasi*, and *Pterosphenus schweinfurthi* in having larger and smaller MTV, respectively; differs from *Pterosphenus kutchensis*, *Pterosphenus schweinfurthi*, and *Pterosphenus schucherti* in weak lateral compression of vertebrae; shares with *Pterosphenus biswasi* and *Pterosphenus schucherti* the presence of paracotylar fossae, but differs from *Pterosphenus schweinfurthi* in lacking paracotylar foramina; differs from *Pterosphenus muruntau* in having synapophyses ventral to the centrum in MTV; differs from *Pterosphenus kutchensis* in the absence of paired synapophyses originating from a common base; differs from *Pterosphenus schweinfurthi*, *Pterosphenus kutchensis*, *Pterosphenus schucherti*, and *Pterosphenus muruntau* in having a trapezoidal neural canal; shares with *Pterosphenus kutchensis* and *Pterosphenus biswasi*, but differs from *Pterosphenus schweinfurthi*, *Pterosphenus schucherti*, and *Pterosphenus muruntau* in having zygosphene as wide as the cotyle; differs from all other *Pterosphenus* species, except *Pterosphenus kutchensis*, in termination of ridge extending from pterapophysis dorsal to the interzygapophyseal ridge and a low PTH/CL ratio; differs from *Pterosphenus biswasi*, *Pterosphenus kutchensis*, *Pterosphenus schweinfurthi*, and *Pterosphenus muruntau* in lacking subcentral foramina.

Occurrence. Harudi Formation, middle Eocene (late Lutetian); Godhatad and Dhedidi North locality, district Kutch, Gujarat state, western India.

Description. The collection comprises 11 well-preserved, associated, partially to nearly complete vertebrae (Figs. 3–6). These are assigned to the precloacal region based on the presence of a hypapophysis and the absence of hemapophyses, pleurapophyses, and lymphapophyses (sensu Rage, 1984). Furthermore, following Parmley and Reed (2003), all specimens in the present study are considered as skeletally mature because of a smaller neural canal relative to the condyle.

The vertebrae, in general, are large (CL = 20–26 mm; Appendix 2) and mediolaterally compressed (PRW/CL = 1–1.1). They are dorsoventrally high (IITR/VPL/SB 3014-1, TVH/CL = 2.1) with the cotyle and condyle arranged along a horizontal axis. The cotyle is deeply concave in anterior view and mediolaterally wider than dorsoventrally high (IITR/VPL/SB 3014-6, COW/COH = 1.2; Figs. 3.1, 3.2, 5.1, 5.2; Appendix 2). It is cordiform in outline with a horizontal to weakly concave dorsal margin and a tapering ventral

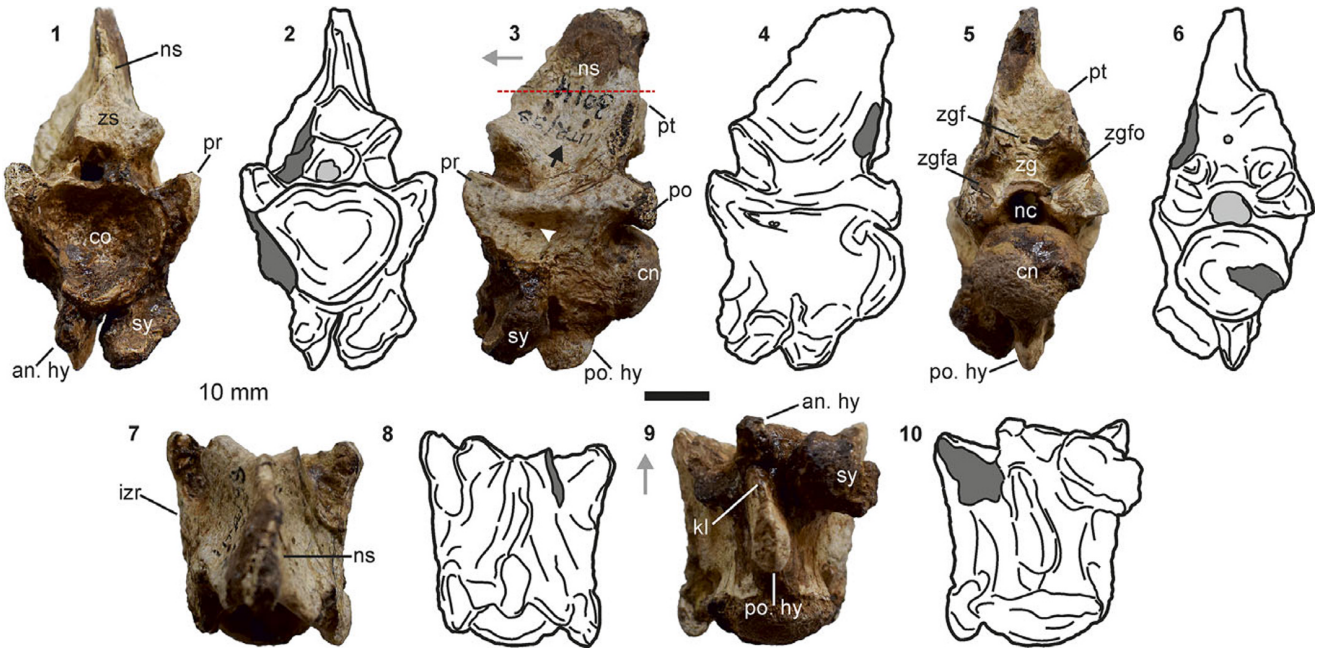

Figure 3. *Pterosphenus rannensis* n. sp., holotype IITR/VPL/SB 3014-1, nearly complete anterior trunk vertebra shown by photographs and interpretative line drawings (in successive order): (**1, 2**) anterior; (**3, 4**) left lateral (white arrowhead and black arrow indicate fossae below interzygapophyseal ridge and at the base of neural spine, respectively); (**5, 6**) posterior; (**7, 8**) dorsal; (**9, 10**) ventral views. Red dashed line marks the dorsal margin of the zygosphene. Gray arrows indicate anterior direction. an.hy = anterior hypapophysis; co = cotyle; cn = condyle; izr = interzygapophyseal ridge; kl = keel; nc = neural canal; ns = neural spine; po = postzygapophysis; po.hy = posterior hypapophysis; pr = prezygapophysis; pt = pterapophysis; sy = synapophysis; zg = zygantrum; zgf = zygantral foramen; zgfa = zygantral facet; zgfo = zygantral fossa; zs = zygosphene. Scale bar = 10 mm.

https://doi.org/10.1017/jpa.2025.10101 Published online by Cambridge University Press

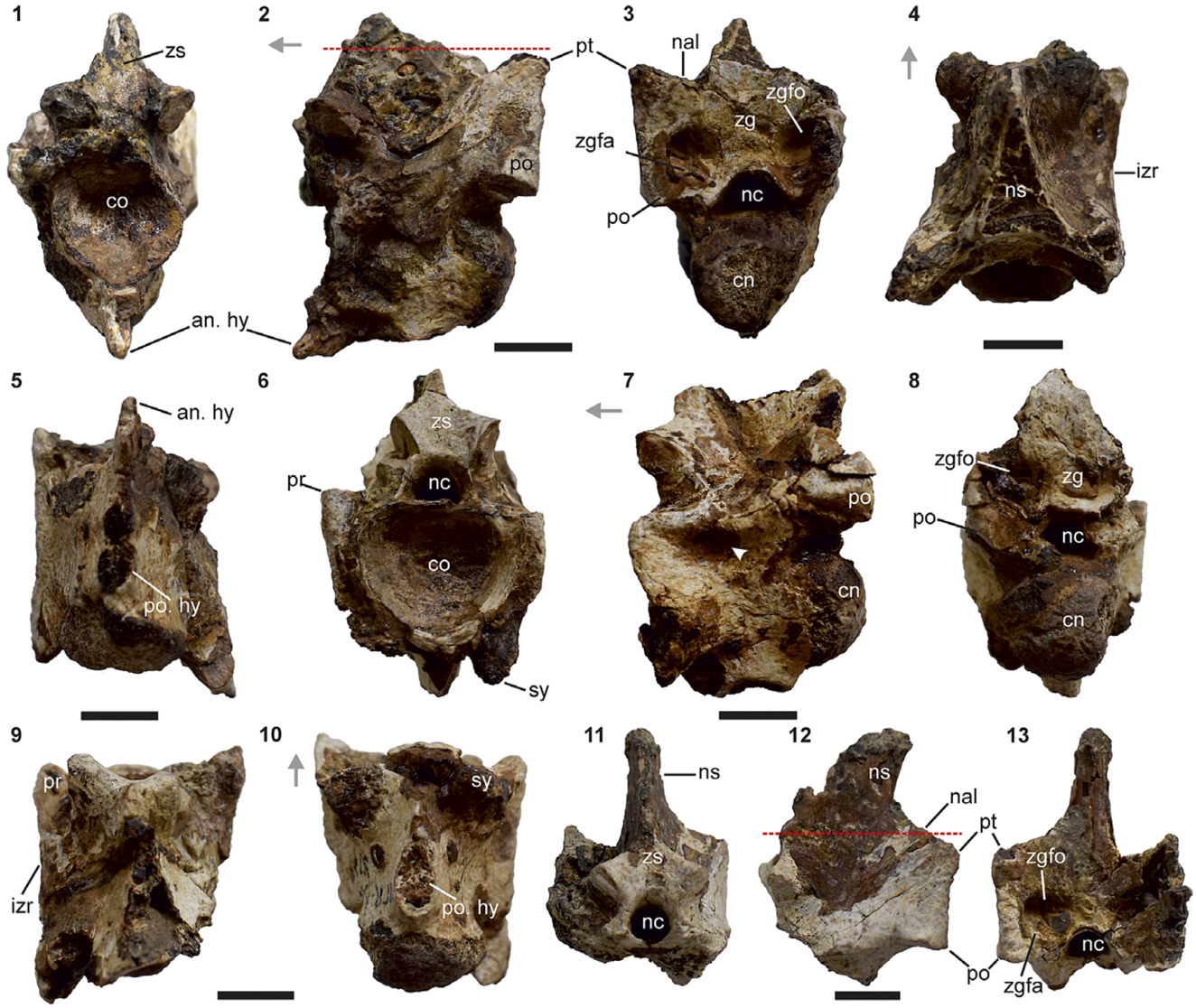

Figure 4. *Pterosphenus rannensis* n. sp.: (**1–5**) holotype IITR/VPL/SB 3014-3, partial anterior trunk vertebra; (**6–10**) holotype IITR/VPL/SB 3014-2, partial ?middle trunk vertebra; and (**11–13**) holotype IITR/VPL/SB 3014-4, partial precloacal neural arch-spine complex: (**1, 6, 11**) anterior, (**2, 7, 12**) left lateral, (**3, 8, 13**) posterior, (**4, 9**) dorsal, and (**5, 10**) ventral views. Red dashed line marks the dorsal margin of the zygosphene. Gray arrows indicate anterior direction. an.hy = anterior hypapophysis; co = cotyle; cn = condyle; izr = interzygapophyseal ridge; nal = neural arch lamina; nc = neural canal; ns = neural spine; po = postzygapophysis; po.hy = posterior hypapophysis; pr = prezygapophysis; pt = pterapophysis; sy = synapophysis; zg = zygantrum; zgfa = zygantral facet; zgfo = zygantral fossa; zs = zygosphene. Scale bars = 10 mm.

margin. This ventral tapering of the cotyle is most prominent in ATV (Figs. 3.1, 4.1). Furthermore, the ventral cotylar rim projects slightly anteriorly relative to the dorsal rim in ATV but is at the same level in MTV. The cotyle is flanked laterally by slender subtriangular paracotylar fossae, which lack paracotylar foramina (Fig. 5.1, 5.2). The condyle, like the cotyle, is mediolaterally wider than high (IITR/VPL/SB 3014-5, CNW/CNH = 1.2; Appendix 2) with a horizontal to weakly concave dorsal and a tapered ventral margin (Fig. 6.3, 6.6).

The synapophysis extends beneath the ventral cotylar rim in all specimens, but its form and position progressively change across the precloacals. In ATV, the synapophysis descends well below the ventral cotylar rim and bears a ventrolaterally directed facet (Fig. 3.1–3.4), whereas in MTV, it is closer to the cotyle with a strongly ventrally directed facet (Figs. 5.1–5.4, 6.1, 6.2). The synapophysis is reniform in lateral/ventrolateral view and lacks a distinct parapophysis and diapophysis (Figs. 3.3, 3.4, 3.9, 3.10, 6.5, 6.8). The ventral half of the synapophysis is deflected anteriorly but does not extend beyond the cotyle.

The prezygapophyseal buttress is vertical and ridge-like, extending from the anterolateral edge of the prezygapophysis to the dorsal margin of the synapophysis. Near its connection with the synapophysis, the buttress is laterally concave (Figs. 3.1, 3.2, 4.6). A prezygapophyseal accessory process is absent and instead, the buttress bears an anterolaterally directed convexity/bulge immediately ventral to the prezygapophyseal articular facet (Figs. 5.1, 5.2, 6.1, 6.2). The orientation of this bulge differs slightly from the anterior to middle trunk vertebrae, being more anteriorly directed in the former.

The prezygapophysis shows a weak dorsolateral lateral deflection in anterior view, with the angle of inclination with the horizontal decreasing from ATV (IITR/VPL/SB 3014-1, PRα = 25°; Fig. 3.1, 3.2) to MTV (IITR/VPL/SB 3014-5, PRα = 9°; Fig. 6.1, 6.4). It is reduced and extends laterally beyond the synapophysis. Relative to the neural

https://doi.org/10.1017/jpa.2025.10101 Published online by Cambridge University Press

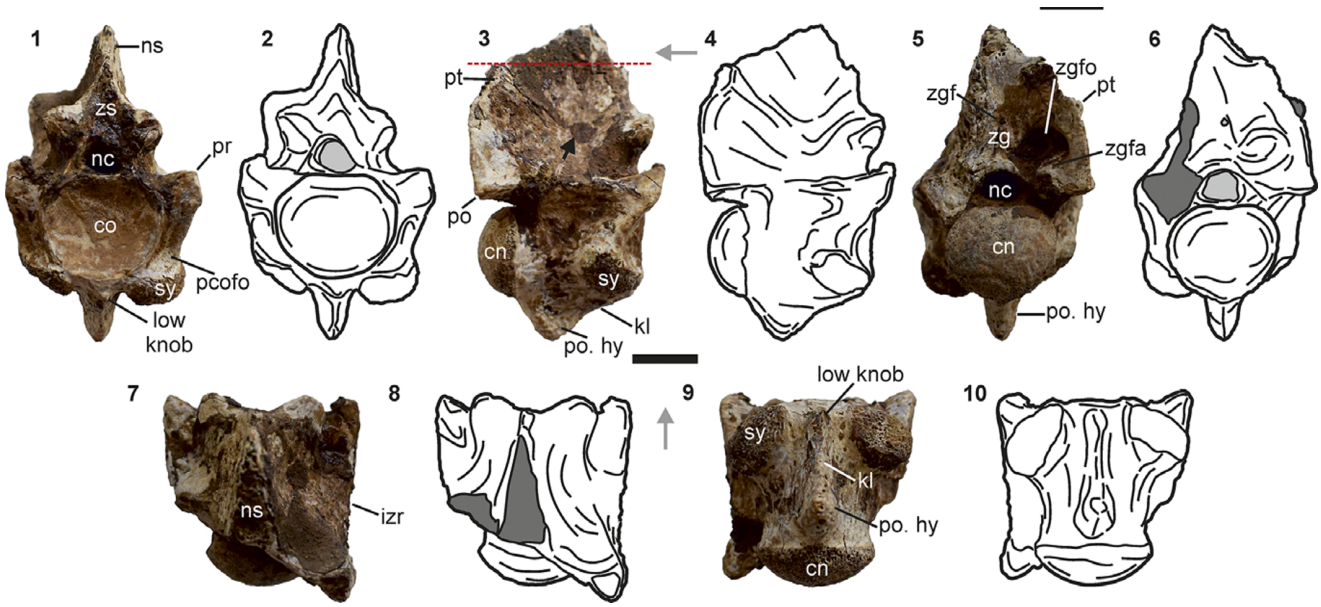

Figure 5. *Pterosphenus rannensis* n. sp., holotype IITR/VPL/SB 3014-5, nearly complete middle trunk vertebra shown by photographs and interpretative line drawings (in successive order): (**1, 2**) anterior; (**3, 4**) right lateral (black arrow indicates fossa at the base of neural spine); (**5, 6**) posterior; (**7, 8**) dorsal; and (**9, 10**) ventral views. Red dashed line marks the dorsal margin of the zygosphene. Gray arrows indicate anterior direction. co = cotyle; cn = condyle; izr = interzygapophyseal ridge; kl = keel; nc = neural canal; ns = neural spine; pcofo = paracotylar fossa; po = postzygapophysis; po.hy = posterior hypapophysis; pr = prezygapophysis; pt = pterapophysis; sy = synapophysis; zg = zygantrum; zgf = zygantral foramen; zgfa = zygantral facet; zgfo = zygantral fossa; zs = zygosphene. Scale bar = 10 mm.

canal, the prezygapophysis remains at the same level as the ventral margin of the canal or rests marginally above the latter (Fig. 5.1, 5.2). The position of the prezygapophysis relative to the neural canal, however, appears higher due to its dorsolateral deflection. In dorsal view, the prezygapophyseal articular facet is triangular (IITR/VPL/SB 3014-1, PRFL/PRFW = 1.5) and anterolaterally deflected from the sagittal plane (Figs. 4.9, 6.7, 6.12). Posterior to the prezygapophysis, the lateral surface of the centrum bears a fossa that is roofed by the interzygapophyseal ridge (Fig. 3.3, 3.4). The postzygapophysis also bears a dorsolateral deflection, but in contrast to the prezygapophysis, the angle of its inclination with the horizontal increases from anterior (IITR/VPL/SB 3014-1, POα = 6°; Fig. 3.5, 3.6) to middle trunk vertebrae (IITR/VPL/SB 3014-7, POα = 16°; Fig. 5.5, 5.6). The postzygapophyseal articular facet is longer than wide (IITR/VPL/SB 3014-1, POFL/POFW = 1.4). In lateral view, the postzygapophysis extends below the level of the prezygapophysis at least in ATV (Fig. 3.3, 3.4). The pre- and postzygapophysis are connected by a sharp and horizontal interzygapophyseal ridge which remains distinct from the pterapophysis throughout its length (Figs. 3.3, 3.4, 5.3, 5.4).

The neural canal is trapezoidal in both anterior and posterior views, and transversely narrower than both the cotyle and zygosphene (Fig. 6.3, 6.4, 6.9, 6.11). The latter is as wide as the cotyle, triangular in anterior view and dorsoventrally high (IITR/VPL/SB 3014-5, MTV, ZSW/COW = 1; ZSH/ZSW = 0.7; Figs. 3.1, 3.2, 4.1, 7, 5.1, 5.2). The anterior surface of the zygosphene accommodates a prominent fossa resulting in a deeply V-shaped embayment, as seen in dorsal view (Figs. 5.7, 5.8, 6.7, 6.12). The concavity of this embayment, however, weakens from ATV (IITR/VPL/SB 3014-1, ZSβ = 115°) to MTV (IITR/VPL/SB 3014-5, ZSβ = 125°). The dorsolateral margin of the zygosphene is concave and anteroventrally directed (Fig. 6.4). The zygosphenal facet is dorsoventrally higher than mediolaterally wide (IITR/VPL/SB 3014-7, ZSFL/ZSFW = 1.2) and anteroventrally deflected so that much of the facet is visible in anterior view. The facet, however, remains posterior to the prezygapophysis. The lateral surface of the neural arch accommodates a shallow fossa between the zygosphene and the pterapophysis at the base of the neural spine (Figs. 3.3, 3.4, 4.12, 5.3, 5.4). This fossa extends slightly below the level of the zygosphene and is flanked ventrally by an anteroventrally directed ridge emanating for the pterapophysis.

The neural arch is strongly vaulted in posterior view with the vaulting ratio (sensu Georgalis et al., 2021b) across the precloacals ranging from 0.8 (ATV) to 0.6 (MTV). The zygantrum is partially roofed and transversely wider than dorsoventrally high (IITR/VPL/SB 3014-4, ZYH/ZYW = 0.2; Figs. 4.3, 4.13, 5.5, 5.6). It accommodates deep bilateral fossae that face posteromedially and are separated by a low median wall (Figs. 3.5, 3.6, 5.5, 5.6). Each fossa comprises an oval, dorsomedially directed zygantral facet. Immediately dorsal to these fossae, a small zygantral foramen in present along the sagittal plane (Figs. 3.5, 3.6, 5.5, 5.6).

The pterapophysis is low and located at ~77% of the total vertebral height (at least in ATV). It is posterodorsally directed in lateral view and remains below the dorsal tip of the zygosphene (Figs. 3.3, 3.4, 4.12, 5.3, 5.4). A mediolaterally compressed and dorsolaterally inclined ridge connects the pterapophysis to the postzygapophysis. Sharp neural arch laminae extend dorsomedially from the pterapophyses to the neural spine. These laminae are concave dorsolaterally with the degree of concavity ranging from 95° (IITR/VPL/SB 3014-3) to 100° (IITR/VPL/SB 3014-4).

The neural spine is mediolaterally compressed and extends to the anterior border of the zygosphene, forming a part of the zygosphenal roof (Figs. 3.1–3.4, 5.1–5.4). It is dorsoventrally high and forms 39% of the total vertebral height in ATV. The spine is subtriangular in lateral view with both the anterior and posterior margins posterodorsally directed.

The ventral surface of the vertebra comprises a large posterior hypapophysis, which is blunt and ventrally directed (Figs. 3.9, 3.10, 6.8). In lateral view, the base of the posterior hypapophysis extends from midlength of the centrum nearly to the ventral condylar rim. A sharp carina/keel extends anteriorly from the posterior

https://doi.org/10.1017/jpa.2025.10101 Published online by Cambridge University Press

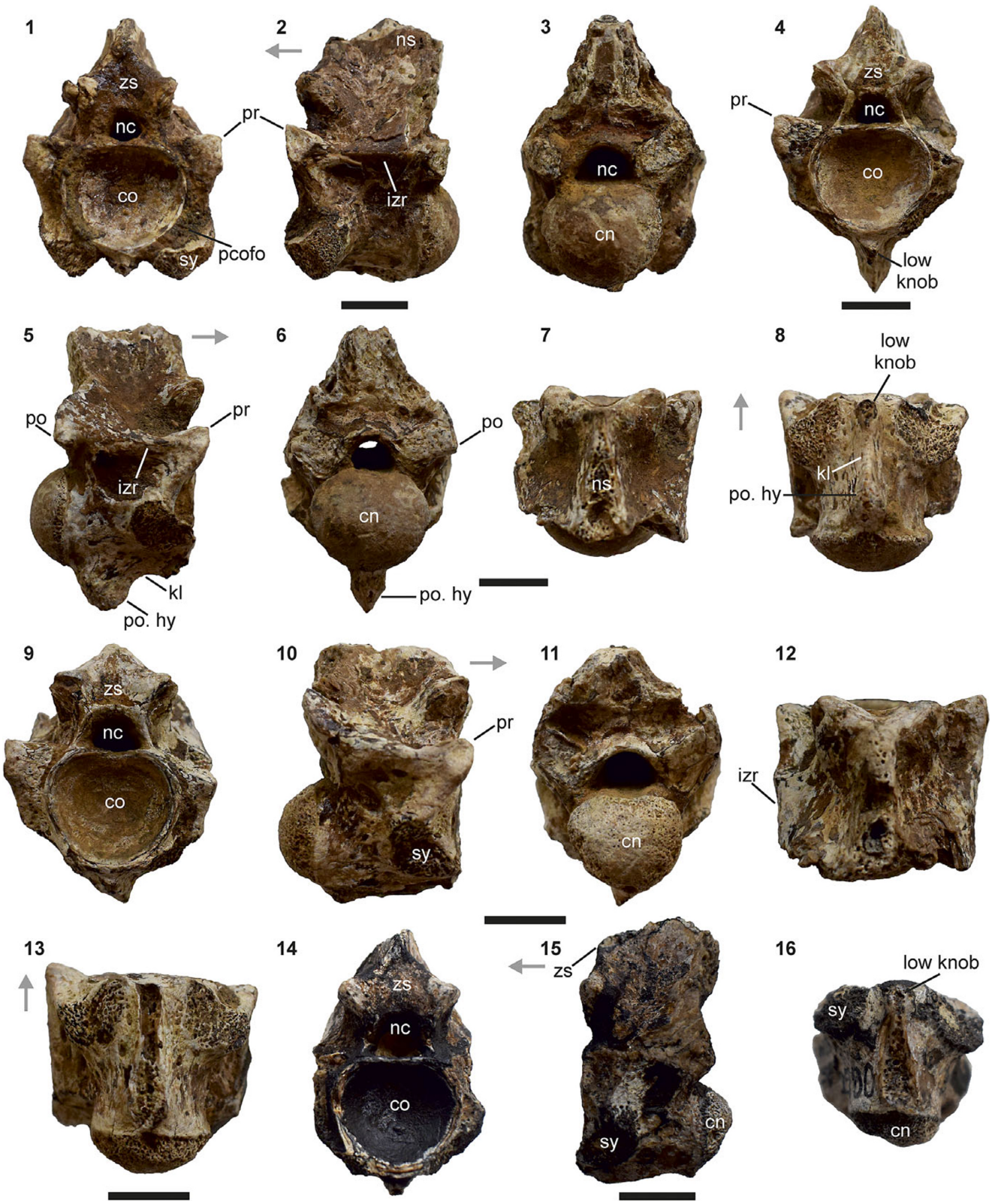

Figure 6. *Pterosphenus rannensis* n. sp.: (**1–3**) holotype IITR/VPL/SB 3014-6, partial middle trunk vertebra; (**4–8**) holotype IITR/SV 3014-7, partial middle trunk vertebra; (**9–13**) holotype IITR/SV 3014-8, partial vertebra; and (**14–16**) IITR/VPL/SB 2980, partial trunk vertebra: (**1, 4, 9, 14**) anterior; (**2, 15**) left lateral; (**3, 6, 11**) posterior; (**5, 10**) right lateral; (**7, 12**) dorsal; and (**8, 13, 16**). Gray arrows indicate anterior direction. co = cotyle; cn = condyle; izr = interzygapophyseal ridge; kl = keel; nc = neural canal; ns = neural spine; pcofo = paracotylar fossa; po = postzygapophysis; po.hy = posterior hypapophysis; pr = prezygapophysis; sy = synapophysis; zs = zygosphene. Scale bars = 10 mm.

https://doi.org/10.1017/jpa.2025.10101 Published online by Cambridge University Press

hypapophysis and gives way to an anteroventrally directed anterior hypapophysis in ATV (Fig. 3.9, 3.10). The anterior hypapophysis is morphologically similar to the posterior hypapophysis, albeit smaller, and is replaced in MTV by a low knob (Figs. 5.1, 5.2, 5.9, 5.10, 6.4, 6.8). Across the precloacals, this ridge connecting the two hypapophyses varies from being dorsal to the synapophysis in ATV (Fig. 3.3, 3.4, 3.9, 3.10) to somewhat ventral in MTV (Fig. 5.3, 5.4, 5.9, 5.10).

In addition to the specimens described above from Godhatad, we report another vertebra (IITR/VPL/SB 2980) of *Pterosphenus rannensis* n. sp. from the Dhedidi locality of the Harudi Formation. IITR/VPL/SB 2980 is missing both the pre- and postzygapophyses, the pterapophyses, and much of the zygantrum and neural spine. Its generic identification is based on the presence of a triangular zygosphene with the preserved anterior margin of the neural spine extending from the dorsal zygosphenal margin (Fig. 6.14, 6.15). The specific attribution is based on the overall morphological similarity of IITR/VPL/SB 2980 with *Pterosphenus rannensis* n. sp. from Godhatad, with the shared presence of a cordiform cotyle that is transversely wider than dorsoventrally high (COW/COH = 1.2), and a zygosphene that is nearly as wide as the cotyle (ZSW/COW = 0.9). Furthermore, IITR/VPL/SB 2980 is most likely from the middle trunk region because the ventral surface of this specimen, although poorly preserved, suggests the presence of a posterior hypapophysis succeeded anteriorly by a low knob rather than an anterior hypapophysis (sensu McCartney and Seiffert, 2016; Fig. 6.16).

Etymology. The specific name is after the Rann of Kutch, referring to the area of geographic origin.

Referred specimen. IITR/VPL/SB 2980, an isolated precloacal vertebra.

Remarks. The diagnostic characters of the new Indian taxon that support its placement within the subfamily Palaeophiinae and the genus *Pterosphenus* are listed above in the Differential diagnosis section (see Rage, 1984; Rage et al., 2003; Houssaye et al., 2013; McCartney and Seiffert, 2016; Georgalis, 2023).

In comparison with the previously recognized species of *Pterosphenus*, *Pterosphenus rannensis* n. sp. (IITR/VPL/SB 3014-5, MTV, CL = 21 mm; PRW = 23.1 mm) is larger than the Indian forms *Pterosphenus kutchensis* (RUSB 2721-1, holotype, MTV, CL = 8.3 mm; PRW = 6.6 mm; Rage et al., 2003) and *Pterosphenus biswasi* (RUSB 2784-4, holotype, MTV, CL = 18.9 mm; PRW = 19.7 mm; Rage et al., 2003), but smaller than the African *Pterosphenus schweinfurthi* (NHMUK PV R 3009b, CL = 33.3 mm, PRW = 29.7 mm). This new taxon is, however, comparable in size to *Pterosphenus schucherti* known from North America (GCVP 19863, MTV, CL = 24.8 mm; PRW = 22.2 mm; Calvert et al., 2022) and now from India (IITBR1/MT1, MTV, CL = 26.72 mm; Natarajan et al., 2024), as well as to the central Asian *Pterosphenus muruntau* (ZIN PC 2/34, paratype, MTV, CL = 23.7; Averianov, 2023).

Contrary to the marked lateral flattening characteristic of *Pterosphenus* vertebrae (Rage et al., 2003; Head et al., 2005; Georgalis, 2023) (e.g., *Pterosphenus kutchensis* [RUSB 2721-1, holotype, MTV, PRW/CL = 0.7; Rage et al., 2003], *Pterosphenus schweinfurthi* [CGM 10194, holotype, TV, PRW/CL = 0.8], *Pterosphenus schucherti* [GCVP 19863, MTV, PRW/CL = 0.8; Calvert et al., 2022]), *Pterosphenus rannensis* n. sp. shows weaker lateral compression (IITR/VPL/SB 3014-6, MTV, PRW/CL = 1.1). The latter feature is reminiscent of 'primitive'-grade *Palaeophis* Owen, 1841 (sensu Rage et al., 2003), e.g., *Palaeophis colossaeus* (MNHN.F.TGE 615, holotype, MTV, PRW/CL = 1.2) and *Palaeophis maghrebianus* (MNHN APH 5, holotype, MTV, PRW/CL = 1.1). A weak lateral compression, however, is also seen in the 'advanced'-grade palaeophiid *Palaeophis typhaeus* ([catalogue number not cited], MTV, PRW/CL = 1.2; Owen, 1850), *Pterosphenus muruntau* (ZIN PH 4/287, ATV, PRW/CL = 1.1; Averianov, 2023) and *Pterosphenus biswasi* (RUSB 2784-4, holotype, MTV, PRW/CL = 1; Rage et al. 2003). *Pterosphenus rannensis* n. sp. shares with *Pterosphenus biswasi* and *Pterosphenus schucherti* (Calvert et al., 2022) the presence of paracotylar fossae. Although this feature is also present in *Pterosphenus schweinfurthi* (see McCartney and Seiffert, 2016), it differs from *Pterosphenus rannensis* n. sp. in bearing paracotylar foramina.

We recognize the weak ventral extension of the synapophyses in MTV of *Pterosphenus rannensis* n. sp. as a distinguishing feature from other *Pterosphenus* species. In taxa such as *Pterosphenus kutchensis*, *Pterosphenus biswasi*, *Pterosphenus schucherti*, and *Pterosphenus schweinfurthi*, the synapophyses in MTV show marked ventral extension relative to the centrum (Rage et al., 2003; Mccartney and Seiffert, 2016; Georgalis, 2023; Natarajan et al., 2024). In *Pterosphenus muruntau*, the synapophyses remain dorsal to the ventral margin of the centrum (Averianov, 2023). Furthermore, the presence of paired synapophyses originating from a common base in *Pterosphenus kutchensis* (see Rage et al., 2003) differentiates the latter from *Pterosphenus rannensis* n. sp. in which this feature is absent. Rage et al. (2003) mentioned the slight ventral displacement of the synapophysis as a characteristic of 'primitive' *Palaeophis* snakes.

The dorsolateral deflection of the pre- and postzygapophysis in *Pterosphenus rannensis* n. sp. contrasts with horizontal zygapophyses in other *Pterosphenus* species, including *Pterosphenus kutchensis*, *Pterosphenus biswasi*, *Pterosphenus schweinfurthi*, and *Pterosphenus schucherti* (Rage et al., 2003; McCartney and Seiffert, 2016; Calvert et al., 2022; Georgalis, 2023). In some specimens of *Pterosphenus schucherti*, however, the prezygapophyses are dorsolaterally deflected (Lucas, 1898; Holman, 1977; Natarajan et al., 2024). *Pterosphenus rannensis* n. sp. shares with *Pterosphenus biswasi* (see Rage et al., 2003) in anterior view a trapezoidal neural canal. This contrasts with the other *Pterosphenus* spp. (*Pterosphenus schweinfurthi*, *Pterosphenus kutchensis*, *Pterosphenus schucherti*, and *Pterosphenus muruntau*) in which the canal is semicircular (Rage et al., 2003; McCartney and Seiffert, 2016; Calvert et al., 2022; Averianov, 2023; Georgalis, 2023).

Pterosphenus rannensis n. sp. (IITR/VPL/SB 3014-5, MTV, NAW/CL = 1) shows weak interzygapophyseal constriction in the middle trunk region, similar to *Pterosphenus schweinfurthi* (DPC 25680, MTV, NAW/CL = 0.9) and *Pterosphenus biswasi* (RUSB 2784-4, holotype, MTV, NAW/CL = 0.9). On the contrary, a stronger interzygapophyseal constriction is seen in *Pterosphenus kutchensis* (RUSB 2721-1, holotype, MTV, NAW/CL = 0.6) and *Pterosphenus schucherti* (GCVP 19863, MTV, NAW/CL = 0.7). A ridge extending anteroventrally from the pterapophysis to the interzygapophyseal ridge distinguishes all species of *Pterosphenus* (McCartney and Seiffert, 2016; Zouhri et al., 2018; Calvert et al., 2022; Averianov, 2023; Georgalis, 2023; Natarajan et al., 2024) except for *Pterosphenus kutchensis* from *Pterosphenus rannensis* n. sp. In the latter Indian forms, this ridge terminates well above the interzygapophyseal ridge.

In *Pterosphenus rannensis* n. sp., the zygosphene is as wide as the cotyle in MTV (IITR/VPL/SB 3014-5, MTV, ZSW/COW = 1), resembling *Pterosphenus kutchensis* (RUSB 2721-1, holotype, MTV, ZSW/COW = ~1) and *Pterosphenus biswasi* (RUSB 2784-4, holotype, MTV, ZSW/COW = ~1). In *Pterosphenus schweinfurthi*

https://doi.org/10.1017/jpa.2025.10101 Published online by Cambridge University Press

(DPC 25680, MTV, ZSW/COW = 1.1) and *Pterosphenus schucherti* (GCVP 19863, MTV, ZSW/COW = 1.1; USNM V 4047, holotype, TV, ZSW/COW = 1.1; IITBR1/MT1, ZSW/ COW = 1.3), the zygosphene is transversely wider, whereas, in *Pterosphenus muruntau* it is narrower (ZIN PC 2/34, holotype, MTV, ZSW/COW = 0.6). *Pterosphenus kutchensis*, however, differs from *Pterosphenus rannensis* n. sp. in the sigmoidal anterior zygosphenal margin and lacking a fossa on the anterior surface of the zygosphene (Rage et al., 2003; McCartney and Seiffert, 2016).

A high vaulting ratio of the neural arch in MTV distinguishes *Pterosphenus kutchensis* (RUSB 2721-1, VR = 1.2) and *Pterosphenus schweinfurthi* (DPC 25680, VR = 0.9) from *Pterosphenus rannensis* n. sp. (IITR/VPL/SB 3014-5, VR = 0.6), *Pterosphenus biswasi* (RUSB 2784-4, VR = 0.7) and *Pterosphenus schucherti* (GCVP 19863, VR = 0.6; IITBR1/MT1, MTV, VR = 0.6) in which this ratio is noticeably lower. A major distinguishing feature between *Pterosphenus rannensis* n. sp. and other *Pterosphenus* species is the height of the pterapophysis relative to both the zygosphene and CL. In *Pterosphenus rannensis* n. sp., the pterapophysis remains below the dorsal tip of the zygosphene on all precloacal vertebrae, and the PTH/CL ratio (0.59–0.62) is low. In all other named species of *Pterosphenus*, the pterapophysis extends above the zygosphene (Holman, 1977; Rage et al., 2003; McCartney and Seiffert, 2016; Averianov, 2023; Georgalis, 2023; Natarajan et al., 2024), and the PTH/CL ratio is significantly higher: *Pterosphenus schucherti* (PTH/CL = 1.3–0.71; see Natarajan et al., 2024, table S3); *Pterosphenus schweinfurthi* (PTH/CL = 1.31–0.82; see Natarajan et al., 2024, table S3), *Pterosphenus muruntau* (PTH/CL = 0.68; see Natarajan et al., 2024, table S3); *Pterosphenus biswasi* (RUSB 2784-4, holotype, MTV, PTH/CL = 0.69; this study). Only in *Pterosphenus kutchinesis* is the PTH/CL ratio (RSUB 2721-1, holotype, MTV, PTH/CL = 0.59; this study) comparable to that in *Pterosphenus rannensis* n. sp. It is noteworthy that the PTH/CL ratio was considered an important distinguishing feature between *Pterosphenus schucherti* and *Pterosphenus muruntau* in a recent study on middle Eocene palaeophiids from India by Natarajan et al. (2024).

The pterapophysis-postzygapohysis connection in *Pterosphenus schucherti*, *Pterosphenus schweinfurthi*, *Pterosphenus kutchensis*, and *Pterosphenus muruntau* shows a well-developed, posteriorly directed concavity in lateral view (Lucas, 1898; McCartney and Seiffert, 2016; Averianov, 2023; Georgalis, 2023; Natarajan et al., 2024). On the contrary, in *Pterosphenus rannensis* n. sp. and *Pterosphenus biswasi*, this connection is vertical/incipiently concave. Furthermore, *Pterosphenus rannensis* n. sp. differs from *Pterosphenus biswasi*, *Pterosphenus kutchensis*, *Pterosphenus schweinfurthi*, and *Pterosphenus muruntau* in lacking subcentral foramina.

It can be noted here that the position of the pterapophysis relative to the zygosphene in *Pterosphenus rannensis* n. sp. is also seen in some 'primitive'- and 'advanced'-grade *Palaeophis* spp. including *Palaeophis colossaeus* (MNHN.F.TGE 615; Georgalis et al., 2021a), *Palaeophis oweni* (MGP-PD 6981Za, 6981Zc; Georgalis et al., 2020), *Palaeophis nessovi* (ZIN PH 16/153; Zvonok and Snetkov, 2012), *Palaeophis casei* (PU 23488; Holman, 1982), *Palaeophis tamdy* Averianov, 1997 (ZIN PH 18/153; Zvonok and Snetkov, 2012), and *Palaeophis littoralis* Cope, 1868 (MSUVP 1212; Parmley and Case, 1988).

The three ecological grades traditionally recognized within Palaeophiinae ('primitive' and 'advanced' *Palaeophis* grade and *Pterosphenus* grade) illustrate a morphological series ranging from species that are weakly adapted to an aquatic habitat to those that are strongly adapted (Rage and Wouters, 1979; Rage et al., 2003). Houssaye et al. (2013), however, considered the segregation of *Palaeophis* species into 'primitive' and 'advanced' grades of no systematic value. Other workers highlighted the lack of a distinct boundary between the two phenotypic genera (*Palaeophis* and *Pterosphenus*) and considered this distinction as possibly artificial (Rage et al., 2003; McCartney et al., 2018; Georgalis et al., 2021a; Smith and Georgalis, 2022; Garberoglio et al., 2024). Fossil evidence showing this indistinctness was previously presented based on material from India and Morocco, in which palaeophiine forms assigned to *Pterosphenus* also preserve features characteristic of *Palaeophis* (Rage et al., 2003; Zouhri et al., 2018). The palaeophiine *Palaeophis nessovi* from Kazakhstan presents a similar pattern because it shows morphological similarity with *Pterosphenus* (Averianov, 1997; Rage et al., 2003; Zouhri et al., 2018). In this context, *Pterosphenus rannensis* n. sp. further adds to the list of palaeophiine taxa that do not completely fit into one of the three ecological grades. The new Indian taxon, although showing features that are diagnostic of *Pterosphenus*, also preserves morphological traits reminiscent of 'primitive' *Palaeophis* species. Nonetheless, based on the zygosphenal and neural spine morphology, we favor placing the new species within *Pterosphenus*. Increased sampling of Eocene deposits in Kutch and other coeval horizons could provide greater anatomical coverage of *Pterosphenus rannensis* n. sp., leading to improved understanding of palaeophiine intracolumnar variation. This, in turn, could provide a better resolution for distinguishing between *Pterosphenus* and *Palaeophis*.

We recognize that the intermediate morphology of the palaeophiines mentioned above and the lack of a clear distinction between *Pterosphenus* and *Palaeophis* present a morphological conundrum. It appears likely that the palaeophiine taxa with such intermediate morphology represent transitional forms between *Palaeophis* and *Pterosphenus*, as suggested by Zouhri et al. (2021). Alternatively, the occurrence of *Palaeophis* features among *Pterosphenus* species and vice versa points to the possibility that some of these morphological features represent ancestral traits of the clade Palaeophiinae. However, in light of the poor understanding of palaeophiine intracolumnar variation, it currently seems premature to prefer one explanation over the other.

Genus ***Palaeophis*** Owen, 1841

Type species. Palaeophis toliapicus Owen, 1841, from the Eocene (Ypresian) of England.

?***Palaeophis* sp. indet.**

Figure 7

Occurrence. Harudi Formation, middle Eocene (late Lutetian); Babia Hill, Kutch district, western India.

Description. IITR/VPL/SB 2632 is an incomplete, isolated vertebra missing the neural spine, left prezygapophysis, left postzygapophysis, and the dorsal tip of the left pterapophysis (Fig. 7). This procoelous vertebra is large (CL = 28 mm; Appendix 2), mediolaterally compressed (PRW/CL = 0.8), and from the middle trunk region. The latter assessment is based on the presence of a large posterior and a smaller peg-like anterior hypapophysis (Fig. 7.1, 7.2, 7.9, 7.10), along with the absence of pleurapophyses, hemapophyses, and lymphapophyses (sensu Rage, 1984; McCartney and Seiffert, 2016).

Both the cotyle and condyle are transversely wider than dorsoventrally high (COW/COH = 1.1, CNW/CNH = 1.1; Appendix 2) and arranged along a horizontal axis. The cotyle is cordiform in

https://doi.org/10.1017/jpa.2025.10101 Published online by Cambridge University Press

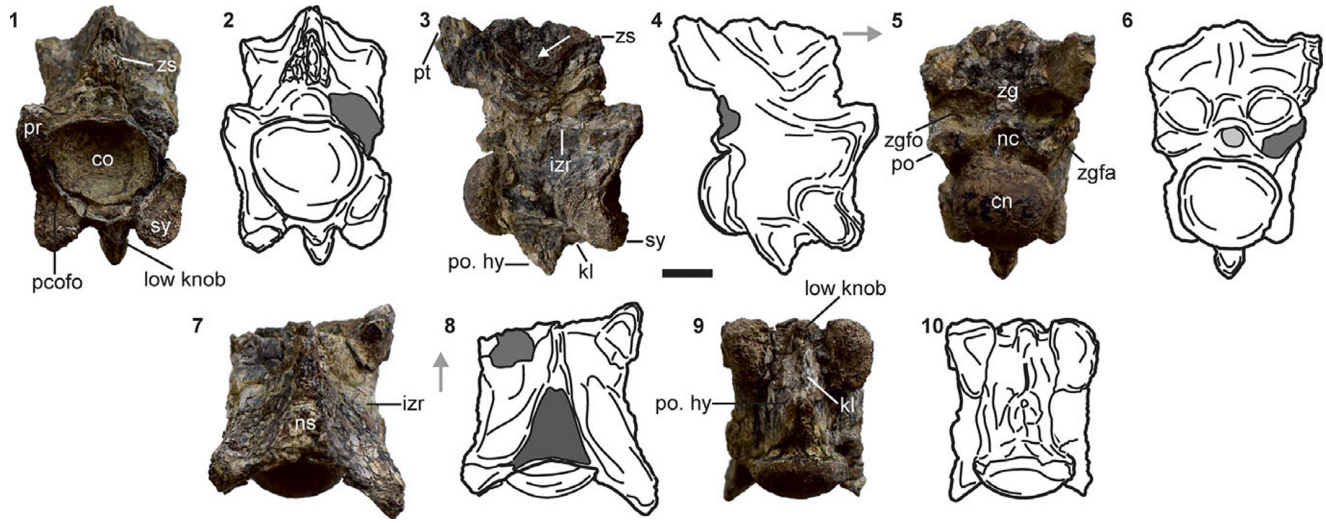

Figure 7. *?Palaeophis* sp. indet., IITR/VPL/SB 2632, nearly complete middle trunk vertebra shown by photographs and interpretative line drawings (in successive order): (**1, 2**) anterior; (**3, 4**) right lateral (white arrow indicates fossa at the base of the neural spine); (**5, 6**) posterior; (**7, 8**) dorsal; and (**9, 10**) ventral views. Gray arrows indicate anterior direction. co = cotyle; cn = condyle; izr = interzygapophyseal ridge; kl = keel; nc = neural canal; ns = neural spine; pcofo = paracotylar fossa; po = postzygapophysis; po.hy = posterior hypapophysis; pr = prezygapophysis; pt = pterapophysis; sy = synapophysis; zg = zygantrum; zgfa = zygantral facet; zgfo = zygantral fossa; zs = zygosphene. Scale bar = 10 mm.

outline whereas the condyle is somewhat triangular (Fig. 7.1, 7.2, 7.5, 7.6). Well-developed paracotylar fossae flank the cotyle laterally but lack paracotylar foramina. The synapophysis is dorsoventrally high and extends well below the ventral margin of the cotyle. It is anteriorly deflected and lacks distinct parapophyseal and diapophyseal facets (Fig. 7.1–7.4).

The prezygapophysis is reduced and strongly deflected dorsolaterally in anterior view (PRα = 39°; Fig. 7.1, 7.2). It extends laterally beyond the synapophysis and is connected to the latter by a mediolaterally compressed prezygapophyseal buttress. The buttress is posteroventrally directed in lateral view and bears an anterolaterally directed, pronounced convexity immediately ventral to the prezygapophyseal articular facet (Fig. 7.1–7.4). The latter is longer than wide in dorsal view (PRFL/PRFW = 1.7) and anterolaterally deflected from the sagittal plane. The prezygapophyseal articular facet rests above the floor of the neural canal for most of its length (in anterior view). However, the medialmost part of the articular facet remains below the canal floor owing to the dorsolateral deflection of the facet. The postzygapophysis is medioventrally deflected (IITR/VPL/SB 2632, POα = 12°), in posterior view (Fig. 7.5, 7.6) and bears a triangular articular facet (IITR/VPL/SB 2632, POFL/POFW = 1.4). The interzygapophyseal ridge is weakly developed and slightly deflected posterodorsally in lateral view (Fig. 7.3, 7.4). The interzygapophyseal constriction is moderate (NAW/CL = 0.8) with the interzygapophyseal ridge being laterally concave in dorsal view.

The anterior surface of the neural arch is badly eroded, obscuring the morphology of the zygosphene and the anterior exit of the neural canal. The eroded zygosphene appears triangular although this could be a preservation artifact. The posterior surface of the neural arch is better preserved and accommodates a subtriangular neural canal, which is succeeded dorsally by a partially roofed zygantrum (Fig. 7.5, 7.6). The zygantral fossae, separated by a low median wall, are deep and posteromedially directed. The zygantral facets, although poorly preserved, appear oval in outline and face dorsomedially. The vaulting ratio (sensu Georgalis et al., 2021b) of the neural arch was found to be high (0.8).

The pterapophysis is well developed, posterodorsally directed, and appears to have extended above the zygosphene, judging from preserved dorsal extent of the latter (Fig. 7.3–7.6). A sharp ridge extends on the anterior surface of the pterapophysis. This ridge turns anteroventrally toward the interzygapophyseal ridge but does not reach it and flanks a shallow fossa medially (Fig. 7.3, 7.4). The pterapophysis is connected to the neural spine by sharp and dorsally concave (θ = 85°) neural arch laminae. Only the base of the neural spine is preserved, which is triangular in cross section and appears to terminate well posterior to the zygophene (Fig. 7.7, 7.8).

The ventral surface of the centrum bears a sharp midline keel that extends between the posterior and anterior hypapophyses (Fig. 7.9, 7.10). The keel is ventrally concave in lateral view and remains dorsal to the ventral margin of the synapophysis (Fig. 7.3, 7.4). The anterior hypapophysis is small and peg-like and bordered laterally by the synapophyses. The large posterior hypapophysis is triangular in lateral view, with a convex posterior and a concave anterior margin. This hypapophysis extends from a short distance anterior to the ventral condylar rim and terminates slightly anterior to the midlength of the centrum.

Materials. IITR/VPL/SB 2632, an isolated middle trunk vertebra.

Remarks. IITR/VPL/SB 2632 is identified as a palaeophiine based on the presence of well-developed pterapophysis, paired hypapophyses, and strong ventral deflection of the synapophyses relative to the centrum (Rage, 1984; Houssaye et al., 2013). When compared with the three palaeophiinae ecological grades proposed by Rage (1984) and Rage et al. (2003), IITR/VPL/SB 2632 shows similarity with 'advanced'-grade *Palaeophis* and *Pterosphenus.* The strong lateral compression of the vertebrae and ventral extent of the synapophysis seen in IITR/VPL/SB 2632 (MTV, PRW/CL = 0.8) resembles those in 'advanced' *Palaeophis* (e.g., *Palaeophis nessovi*, ZIN PH 119, MTV, PRW/CL = 0.8), *Pterosphenus* (e.g., *Pterosphenus kutchensis* [RUSB 2721-1, holotype, MTV, PRW/CL = 0.7; Rage et al., 2003], and *Pterosphenus schweinfurthi* [DPC 25680, MTV, PRW/CL = 0.9; McCartney and Seiffert, 2016; Georgalis, 2023]). This Indian palaeophiine (IITR/VPL/SB 2632, MTV,

https://doi.org/10.1017/jpa.2025.10101 Published online by Cambridge University Press

PRFL/CL = 0.3) also shares a marked reduction of the prezygapophyses with these two ecological grades (e.g., *Pterosphenus schweinfurthi* [e.g., DPC 25680, MTV, PRFL/CL = ~0.3], *Pterosphenus schucherti* [GCVP 19863, MTV, PRFL/CL = 0.3], *Palaeophis nessovi* [ZIN PH 119, MTV, PRFL/CL = ~0.3], *Palaeophis* cf. *Palaeophis toliapicus* from Crimea [ZIN PH 14/153, PRFL/CL = 0.2]). The dorsal extent of the pterapophysis in IITR/VPL/SB 2632 is similar to that of *Pterosphenus* (e.g., *Pterosphenus schweinfurthi*, *Pterosphenus schucherti*, *Pterosphenus muruntau*, *Pterosphenus kutchensis*), whereas its neural spine morphology is characteristic of *Palaeophis* because it remains distinct from the zygosphene (Rage, 1984; Rage et al., 2003; Houssaye et al., 2013; McCartney and Seiffert, 2016; Georgalis et al., 2021a; Averianov, 2023; Georgalis, 2023).

The discussion above suggests that IITR/VPL/SB 2632 had clear adaptations for an aquatic life considering its similarities with 'advanced'-grade *Palaeophis* and *Pterosphenus* snakes (sensu Rage et al., 2003). Although most features characterizing IITR/VPL/SB 2632 are common to the two aforementioned ecological grades, the termination of the neural spine posterior to the zygosphenal roof suggests referral of this Indian palaeophiine to *Palaeophis* (sensu Rage, 1984; Rage et al., 2003; Houssaye et al., 2013). In light of the poorly preserved zygosphene, the neural spine morphology of IITR/VPL/SB 2632 is possibly the only feature indicative of its generic affinity. Furthermore, the vertebral morphology of IITR/VPL/SB 2632 also highlights its distinctiveness from *Pterosphenus rannensis* n. sp. Although IITR/VPL/SB 2632 is of the same geological age as *Pterosphenus rannensis* n. sp., it differs from the latter taxon in having stronger lateral vertebral compression, greater ventral extent of synapophysis, pterapophysis extending above zygosphene, and the neural spine distinct from the zygosphene. Although the morphological comparison of IITR/VPL/SB 2632 with the palaeophiine ecological grades and *Pterosphenus rannensis* n. sp. suggests the presence of a second middle Eocene palaeophiine taxon in Kutch, we refrain from naming IITR/VPL/SB 2632 because of limited material currently available and instead refer to it as ?*Palaeophis* sp. indet.

Genus ***Pterosphenus*** Lucas, 1898

Type species. *Pterosphenus schucherti* Lucas, 1898, from the late Lutetian or early Bartonian, and Priabonian, USA.

Pterosphenus biswasi Rage et al., 2003
Figure 8

Holotype. RUSB 2784-4, partial trunk vertebra.

Revised Diagnosis. *Pterosphenus biswasi* is diagnosed based on a unique combination of the following features: transversely wide trunk vertebrae (differs in this respect from *Pterosphenus schucherti*,

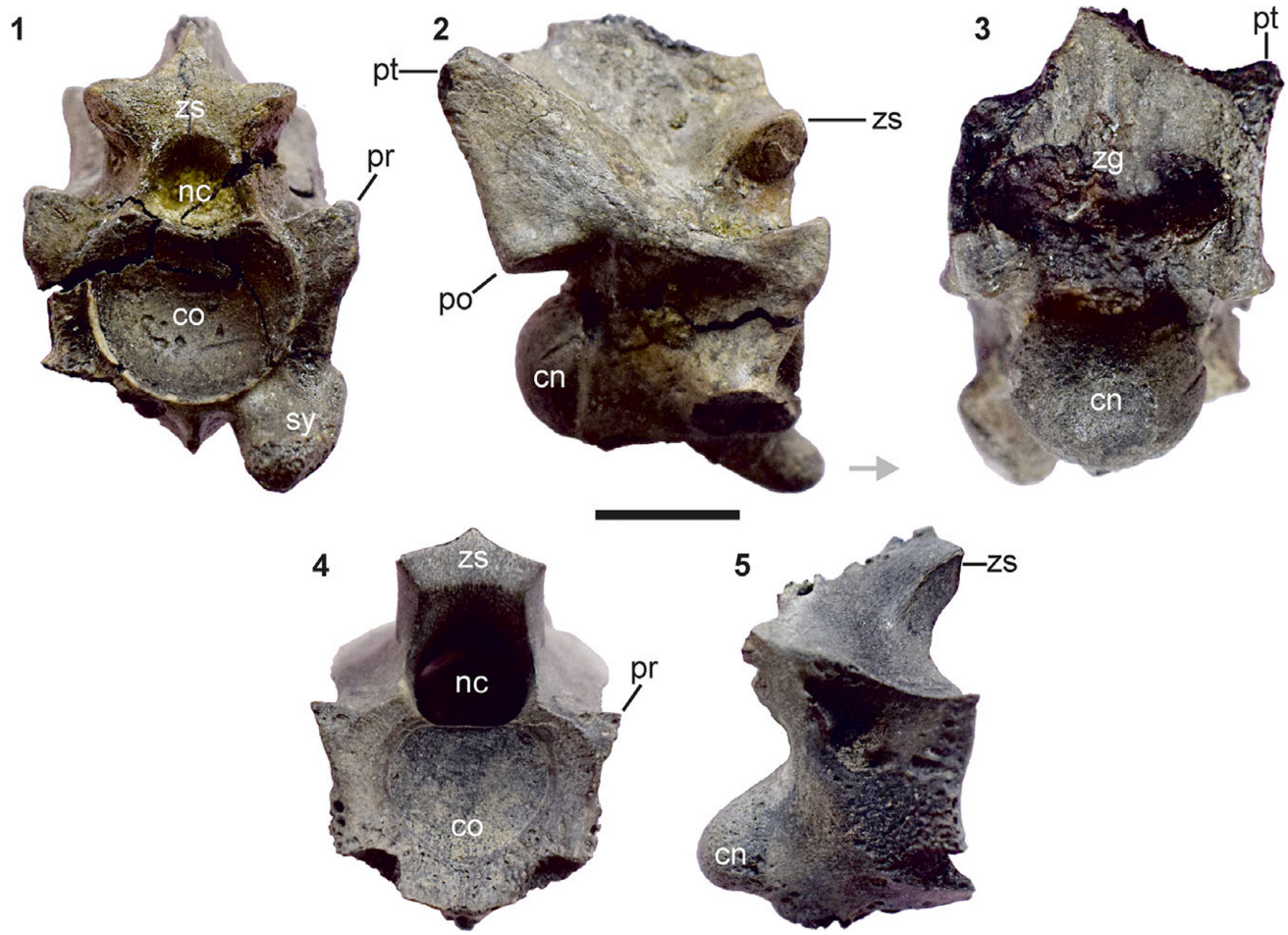

Figure 8. *Pterosphenus biswasi* Rage et al., 2003: (**1–3**) holotype RUSB 2784-4, partial middle trunk vertebra; (**4, 5**) RUSB 2565-1, partial trunk vertebra: (**1, 4**) anterior; (**2, 5**) right lateral; and (**3**) posterior. Gray arrow indicates anterior direction. co = cotyle; cn = condyle; nc = neural canal; po = postzygapophysis; pr = prezygapophysis; pt = pterapophysis; sy = synapophysis; zg = zygantrum; zs = zygosphene. Scale bar = 10 mm.

https://doi.org/10.1017/jpa.2025.10101 Published online by Cambridge University Press

Pterosphenus schweinfurthi, and *Pterosphenus kutchensis*); synapophyses separated by anterior hypapophysis (differs from *Pterosphenus kutchensis*); synapophyses extendind below ventral cotylar rim (differs from *Pterosphenus muruntau*); pterapophysis dorsoventrally low, extending slightly above zygosphene (differs from *Pterosphenus schucherti*, *Pterosphenus schweinfurthi*, and *Pterosphenus rannensis* n. sp.); weakly concave pterapophyseal-postzygapophyseal connection (differs from *Pterosphenus muruntau*, *Pterosphenus schucherti*, and *Pterosphenus schweinfurthi*).

Referred specimen. Partial trunk vertebrae (RUSB 2565-1, 2790-21).

Remarks. *Pterosphenus biswasi* was originally described by Rage et al. (2003), together with the highly distinct *Pterosphenus kutchensis*, from the early Lutetian lignite deposits of Kutch (see Datta and Bajpai, 2024, supplementary note 1). Rage et al. (2003) distinguished the two taxa based on the presence of an anterior hypapophysis in *Pterosphenus biswasi* along with short and separated synapophyses and a concave anterior margin of the zygosphene. The latter taxon was further distinguished from *Pterosphenus schucherti* and *Pterosphenus schweinfurthi* by a shallower concavity of the anterior zygosphenal margin and a higher zygosphenal plane. Recently, however, Natarajan et al. (2024) synonymized *Pterosphenus biswasi* with *Pterosphenus schucherti*. These authors, while describing vertebrae attributed to *Pterosphenus schucherti* from the late Lutetian of Kutch, considered the previously listed features distinguishing *Pterosphenus biswasi* from *Pterosphenus schucherti* as nondiagnostic due to intra- and intercolumnar variation.

Here, we reassess the holotype and referred specimens of *Pterosphenus biswasi* (Fig. 8), considering its validity in the diversity of Indian palaeophiines and the stratigraphic range and evolution of *Pterosphenus schucherti*. Our observations find marked differences between *Pterosphenus biswasi* and *Pterosphenus schucherti*/*Pterosphenus schweinfurthi* with regard to the pterapophyseal morphology and overall form. Unlike *Pterosphenus schucherti* (IITBR1/AT5, ATV, PRW/CL = 0.8; GCVP 19863, MTV, PRW/CL = 0.8; Calvert et al., 2022) and *Pterosphenus schweinfurthi* (CGM 10194, holotype, TV, PRW/CL = 0.8) in which the vertebrae show strong lateral compression, the vertebrae of *Pterosphenus biswasi* are transversely wider (RUSB 2784-4, holotype, MTV, PRW/CL = 1; RUSB 2565-1, TV, PRW/CL = 1.12; Rage et al., 2003). The pterapophysis in *Pterosphenus biswasi* is dorsoventrally low and extends only for a short distance above the zygosphene (RUSB 2784-4, holotype, MTV, PTH/CL = 0.69, PT. VH/ZS. VH = 1; see Fig. 2). In both *Pterosphenus schucherti* (PTH/CL = 1.3–0.71, mean 1.1; see Natarajan et al., 2024, table S3; IITBR1/AT1–MT1, PT. VH/ZS. VH = 1.2–1.6) and *Pterosphenus schweinfurthi* (PTH/CL = 1.31–0.82, mean 1.2; see Natarajan et al., 2024, table S3; CGM 10194, holotype, TV, PT. VH/ZS. VH = 1.2; NHMW 2010/0188/0001d, TV, PT. VH/ZS. VH = 1.2), the pterapophyses are high and extend well above the zygosphene. Additionally, a weakly concave pterapophyseal-postzygapophyseal connection in *Pterosphenus biswasi* distinguishes it from *Pterosphenus schucherti*/*Pterosphenus schweinfurthi* in which this connection is markedly concave (Lucas, 1898; Andrews, 1901; McCartney and Seiffert, 2016; Georgalis, 2023; Natarajan et al., 2024). Although a low PTH/CL ratio similar to that in *Pterosphenus biswasi* is also seen in *Pterosphenus muruntau* (PTH/CL = 0.68; see Natarajan et al., 2024, table S3), the latter taxon is distinguished by a higher PT. VH/ZS. VH ratio (1.4), zygosphene narrower than cotyle (ZIN PC 2/34, holotype, MTV, ZSW/COW = 0.6), and synapophysis placed dorsal to ventral cotylar rim in MTV and marked concavity of pterapophyseal-postzygapophysis connection (see Averianov, 2023).

In light of these morphological differences, we reassert the validity of *Pterosphenus biswasi*. Although the validity of some features (e.g., orientation of synapophysis, shape of posterior hypapophysis, inclination of pterapophysis and neural spine, concavity of zygosphene, width of neural canal, and height of zygapophyseal plane) traditionally used to differentiate palaeophiine taxa have been questioned (Georgalis et al., 2020; Georgalis, 2023; Natarajan et al., 2024), we consider the pterapophyseal morphology and the extent of lateral vertebral compression in *Pterosphenus biswasi* as robust diagnostic features. Indeed, both features have been repeatedly used by previous workers to differentiate palaeophiine taxa (e.g., Georgalis et al., 2020; Georgalis, 2023; Aniny et al., 2024; Garberoglio et al., 2024). The extent of vertebral compression is also considered among the key features defining the three palaeophiine ecological grades proposed by Rage (1984) and Rage et al. (2003). It is noteworthy that the height of the pterapophysis and its ratio to centrum length (PTH/CL), in particular, were used by Natarajan et al. (2024) to not only assign their specimens to *Pterosphenus schucherti* but also to distinguish the latter from *Pterosphenus muruntau* and *Pterosphenus sheppardi*. Natarajan et al. (2024), however, did not evaluate the pterapophyseal height or the degree of vertebral compression of *Pterosphenus biswasi* when synonymizing it with *Pterosphenus schucherti*.

Family **Madtsoiidae** Hoffstetter, 1961

Madtsoiidae gen. indet. sp. indet.

Figure 9

Occurrence. Naredi Formation, middle Eocene (early Lutetian); Panandhro Lignite Mine, Kutch district, Gujarat state, western India.

Description. IITR/VPL/SB 2782 is an isolated nearly complete vertebra (Fig. 9) missing only the left zygosphenal facet and parapophysis. The specimen possibly represents a middle trunk vertebra based on the absence of a hypapophysis, pleurapophyses, and lymphapophyses, and a wider neural arch relative to centrum length (sensu Rage, 1984; LaDuke et al., 2010; Rio and Mannion, 2017).

The vertebra is massive with a centrum length (CL) and prezygapophyseal width (PRW) of 67.9 mm and 95.8 mm, respectively (Appendix 2). The centrum is procoelous with the cotyle and condyle deflected anteroventrally and posterodorsally, respectively. The cotyle is concave in anterior view and transversely wider than dorsoventrally high (COW/COH = 1.2; Fig. 9.1). It is bordered laterally by well-developed paracotylar fossae. The dorsal and ventral margins of the fossa are defined by bony struts extending from the dorsolateral and lateral cotylar margins, respectively. A secondary, weak bony strut, arising from the dorsolateral margin of the cotyle, further divides the paracotylar fossa into a deeper ventral and a shallower dorsal portion. The latter accommodates a large paracotylar foramen beside the lateroventral margin of the neural canal (Fig. 9.1). The condyle, similar to the cotyle, is mediolaterally wider than dorsoventrally high (CNW/CNH = 1.1; Fig. 9.3).

The synapophysis is dorsoventrally high and ventrolaterally inclined in anterior view (SYα = 64°). In lateral view, the synapophysis is reniform in outline and inclined at 30° from the vertical plane. A distinct diapophysis and parapophysis are present (Fig. 9.2). The parapophyseal facet is subrectangular in lateral view and remains dorsal to the ventral cotylar rim. A prominent paracotylar notch separates the parapophysis from the cotyle (Fig. 9.1).

https://doi.org/10.1017/jpa.2025.10101 Published online by Cambridge University Press

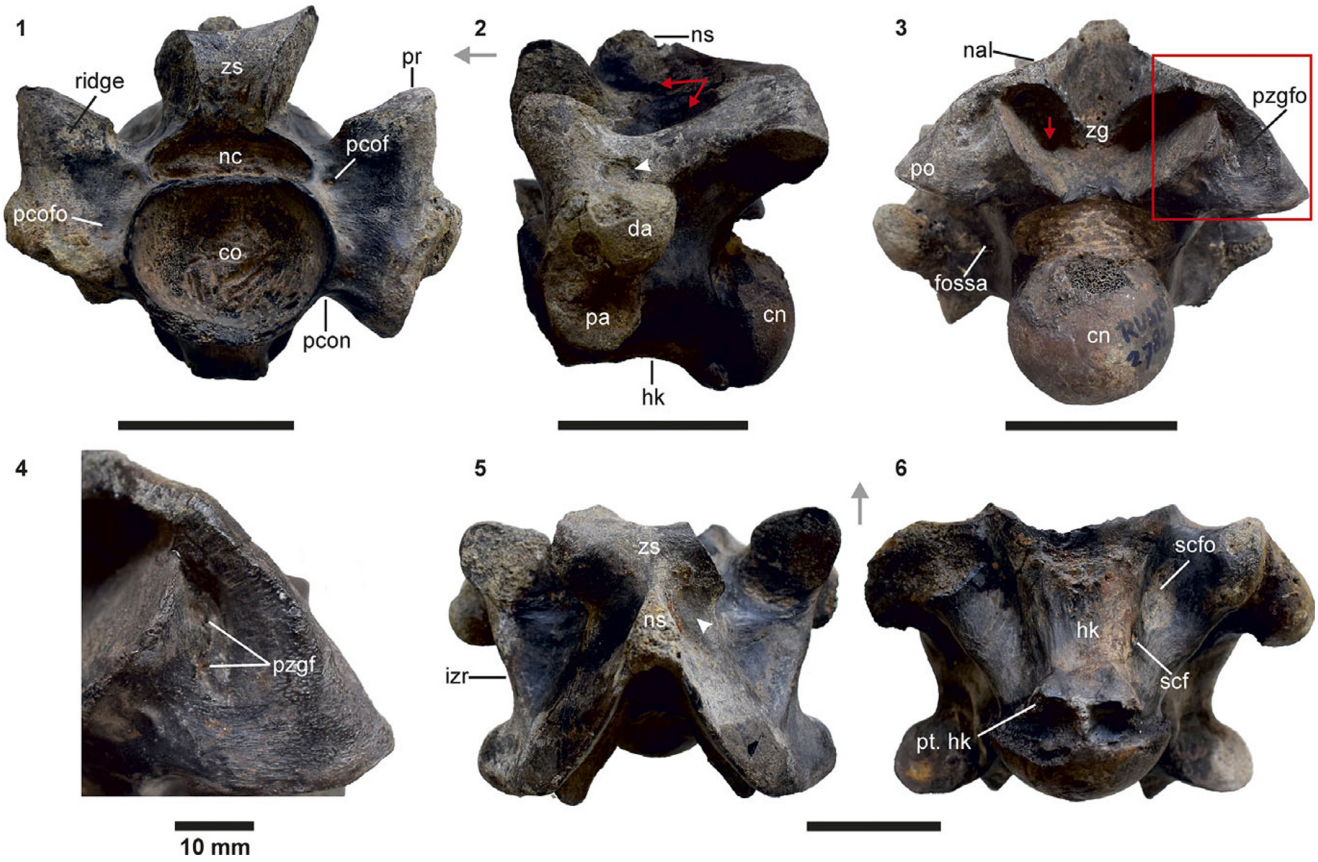

Figure 9. Madtsoiidae gen. indet. sp. indet., IITR/VPL/SB 2782, nearly complete middle trunk vertebra: (**1**) anterior; (**2**) left lateral (red arrows indicate fosse above and below bony strut extending posteriorly from the zygosphene; white arrowhead indicates fossa medial to diapophysis); (**3**) posterior (red arrow indicates endozygantral foramen); (**4**) inset of **9.3** at higher magnification showing paired parazygantral foramina on right parazygantral fossa; (**5**) dorsal (white arrowhead indicates fossa above bony strut extending posteriorly from the zygosphene); and (**6**) ventral views. Gray arrows indicate anterior direction. co = cotyle; cn = condyle; da = diapophysis; hk = hemal keel; izr = interzygapophyseal ridge; nal = neural arch lamina; nc = neural canal; ns = neural spine; pa = parapophysis; pcof = paracotylar foramen; pcofo = paracotylar fossa; pcon = paracotylar notch; po = postzygapophysis; pr = prezygapophysis; pt.hk = posterior terminus of hemal keel; pzgf = parazygantral foramen; pzgfo = parazygantral fossa; scf = subcentral foramen; scfo = subcentral fossa; zg = zygantrum; zs = zygosphene. Scale bars = 50 mm (except as noted).

The diapophysis is bulbous and posterodorsally directed in lateral view. It extends beyond the prezygapophysis in anterior view. The dorsal margin of the diapophysis remains ventral to the dorsal cotylar rim. A large fossa is present on the lateral surface of the centrum posterior to the paradiapophysis (Fig. 9.3).

The prezygapophyseal buttress is massive and bears a weakly raised oblique ridge on its anterior surface (Fig. 9.1). A prezygapophyseal accessory process is absent and the buttress is succeeded posteriorly by a deep, elliptical fossa (Fig. 9.2). The latter is roofed by the interzygapophyseal ridge and lies medial to the diapophysis on the lateral surface of the centrum. Both the pre- and postzygapophyses are medioventrally inclined (IITR/VPL/SB 2782, PRα = 35°, POα = 31°) in anterior and posterior views (Fig. 9.1, 9.3), respectively, and bear subelliptical facets (IITR/VPL/SB 2782, PRFL/PRFW = 1.2, POFL/POFW = 1.1). In dorsal view, the prezygapophyseal articular facets are obliquely oriented at an angle of 46° to the sagittal plane, and, in anterior view, the prezygapophyses extend well above the dorsal margin of the neural canal. The interzygapophyseal ridge is robust and extends posterodorsally from the pre- to the postzygapophysis. In dorsal view. the ridge is largely straight except for a weak lateral convexity near the prezygapophysis (Fig. 9.5).

The neural canal is transversely wider than dorsoventrally high (IITR/VPL/SB 2782, NCW/NCH = 1.9; Fig. 9.1) and reniform in outline. The width of the canal resembles that of the zygosphene but is slightly less than that of the cotyle. The trapezoidal zygosphene (Fig. 9.1) is mediolaterally wider than dorsoventrally high (IITR/VPL/SB 2782, ZSW/ZSH = 1.4) and comprises a large oval facet (IITR/VPL/SB 2782, ZSFL/ZSFW = 0.9). The dorsal margin of the zygosphene is concave in anterior view, and the facet is steeply inclined (22° from the vertical). In dorsal view, the anterior zygosphenal margin is notched (ZSβ = 92°; Fig. 9.5). The zygantrum is transversely wide and comprises subelliptical facets (Fig. 9.3). The latter are steeply inclined (30° from the vertical) and accommodate paired endozygantral foramina that open posterodorsally. The zygantral roof above each facet is dorsomedially convex, and the two roofs converge along the midline to form a U-shaped embayment. The zygantrum is flanked laterally by prominent parazygantral fossae, where the left fossa accommodates two small parazygantral foramina (Fig. 9.3, 9.4).

The neural spine is dorsoventrally low (IITR/VPL/SB 2782, NSH/TVH = 0.09; Fig. 9.2) and vertically oriented. The anterior spinal margin is posterodorsally directed, whereas the posterior margin is straight and the cross section of the spine approximates the shape of an arrowhead (Fig. 9.5). The spine is buttressed posteriorly by neural arch laminae that extend posteroventrally from the dorsal margin of the neural spine to the dorsolateral margin of the postzygapophyses and enclose a deep median

https://doi.org/10.1017/jpa.2025.10101 Published online by Cambridge University Press

embayment (Fig. 9.3). The latter is mediolaterally compressed in dorsal view, with the laminae diverging at an angle of 51°. The neural spine is bound on either side by a shallow, elongated fossa (Fig. 9.2, 9.5). The latter is placed immediately posterior to the zygosphene and bordered by ventrally rounded bony struts extending from the posterolateral margin of the zygosphene. Ventral to these struts, the dorsal surface of the neural arch bears triangular fossae, with the apex of the triangle directed posteriorly (Fig. 9.2).

The centrum is triangular in ventral view and widest across the parapophyses (Fig. 9.6). Much of the ventral surface of the centrum is occupied by anteroposteriorly elongated paired subcentral fossae, which are bordered laterally by subcentral ridges. The ridges are robust and sinuous, extending posteromedially from the parapophyses to the dorsoventral midpoint of the condyle. A broad and transversely convex hemal keel separates the subcentral fossae. This keel terminates anterior to the precondylar constriction and is connected to the condyle by a sharp ridge (Fig. 9.6). At its posterior terminus, the hemal keel is chisel-shaped with sharp posteroventrally directed protuberances. Small subcentral foramen is present on either side of the hemal keel. The hemal keel, in lateral view, descends well below the level of the parapophysis (Fig. 9.2).

Material. IITR/VPL/SB 2782, a nearly complete middle trunk vertebra.

Remarks. IITR/VPL/SB 2782 is identified as a madtsoiid based on a unique combination of the following characters: presence of paracotylar and parazygantral fossae and foramina, diapophysis extending beyond the lateral margin of the prezygapophysis, prominent hemal keel with paired projections at posterior terminus, and prezygapophyseal accessory process absent. The generic affinity of this specimen was also evaluated, and in view of its large size (CL = 67.9 mm, PRW = 96.3 mm), comparisons were made with the only two large-bodied madtsoiids (*Vasuki indicus* and *Platyspondylophis tadkeshwarensis*) known from the Eocene of India (Smith et al., 2016; Datta and Bajpai, 2024).

We consider the referral of IITR/VPL/SB 2782 to the stratigraphically older *Platyspondylophis* (~55 Ma) unlikely because of the significantly smaller size (CL = 18–21 mm; PRW = 26–43 mm; Smith et al., 2016) and the lack of both paracotylar and parazygantral foramina in the latter taxon. *Platyspondylophis* further differs from IITR/VPL/SB 2782 in bearing arcuate interzygapophyseal ridges and transverse prezygapophyseal facets, visible in dorsal view, a trilobate neural canal, an unnotched zygosphene, and a dorsoventrally higher neural spine (see Smith et al., 2016). On the other hand, referral of IITR/VPL/SB 2782 to *Vasuki* seems most likely because the two were found at the same fossil locality. This referral is further supported by the following features shared by IITR/VPL/SB 2782 with the MTV of *Vasuki*: comparable vertebral size; cotyle and condyle transversely wider than high (IITR/VPL/SB 2782, COW/COH = 1.2, CNW/CNH = 1.1); moderately deep paracotylar fossae that are weakly subdivided into deeper ventral and shallower dorsal parts; high synapophyseal angle (IITR/VPL/SB 2782, SYα = 64°) and distinct para- and diapophyseal facts; moderately inclined pre- and postzygapophysis in anterior and posterior views, respectively (PRα = 35°, POα = 31°); reniform neural canal; trapezoidal, transversely wider than high zygosphene (IITR/VPL/SB 2782, ZSW/ZSH = 1.4); deep fossa medial to the diapophysis; large subcentral fossae with prominent subcentral foramina.

Nevertheless, a cohort of features distinguish this middle trunk vertebra (IITR/VPL/SB 2782) from those of *Vasuki indicus*. These include the presence of two parazygantral foramina on the right parazygantral fossa, larger paracotylar foramina, ventral position of the diapophysis relative to the dorsal cotylar rim, strongly notched anterior zygosphenal margin (IITR/VPL/SB 2782, ZSβ = 92°), weaker angle of divergence of the neural arch laminae (51°), absence of a prespinal lamina, and extension of the hemal keel below the parapophyses. These differences suggest the possible presence of a second large madtsoiid in the middle Eocene of Kutch. We consider the differences between IITR/VPL/SB 2782 and *Vasuki* as taxonomically significant and not intracolumnar variation because these differences are consistently present in all MTV of *Vasuki indicus*. In view of the morphological similarities and differences between *Vasuki* and IITR/VPL/SB 2782, the latter possibly represents a new species of *Vasuki*. Alternatively, the morphological differences in IITR/VPL/SB 2782 might reflect sexual dimorphism. LaDuke (1991) reported sexual dimorphism in *Thamnophis sirtalis sirtalis* Linnaeus, 1758 based on the relative size of the cotyle and condyle, with these features being larger in females. In IITR/VPL/SB 2782, however, the proportions of the cotyle and condyle resemble those in *Vasuki*. For these reasons and in view of the limited material currently available as well as a lack of knowledge of sexual dimorphism in madtsoiids, we refrain from naming a new species at this time.

Family **?Nigerophiidae** Rage, 1975
?Nigerophiidae gen. indet. sp. indet.
Figures 10, 11

Occurrence. Naredi Formation, Kutch district, Gujarat state, western India; early Eocene (Ypresian).

Description. IITR/VPL/SB 97 (Fig. 10) is an isolated vertebra missing the right prezygapophysis, left postzygapophysis, and part of the zygosphene and neural spine-arch complex. Based on the presence of a hypapophysis, and absence of hemapophyses, pleurapophyses, and lymphapophyses, this specimen is assigned to the precloacal region (sensu Rage, 1984).

The vertebra is small (CL = 10.16 mm, PRW = ~10.9 mm; Appendix 2), mediolaterally compressed (PRW/CL = 1.1), and dorsoventrally high (TVH/PRW = 1.2). The cotyle is subcircular (COW/COH = 1.1) and bordered laterally by crescentic paracotylar fossae (Fig. 10.1, 10.2). These fossae are moderately deep and separated from the ventrolateral margins of the neural canal by prominent ridges. A small paracotylar foramen is present only in the left paracotylar fossa. The condyle, similar to the cotyle, is nearly circular (CNW/CNH = ~1; Fig. 10.3, 10.4). The synapophysis is ventrolaterally directed and extends slightly beyond the ventral margin of the centrum (Fig. 10.1, 10.2). Distinct parapophyseal and diapophyseal facets are not discernible.

The prezygapophysis is nearly horizontal in anterior view (PRα = 5°) and rests slightly above the ventral rim of the neural canal (Fig. 10.1, 10.2). It is laterally directed, although in dorsal view, the prezygapophysis is strongly deflected anterolaterally. The prezygapophyseal articular facet is triangular (PRFL/PRFW = 2.4). The prezygapophyseal buttress is a sharp, anterolaterally convex ridge. The postzygapophysis is weakly inclined medioventrally in posterior view and bears a subelliptical facet (POFL/POFW = 1.1; Fig. 10.3, 10.4). It is connected to the prezygapophysis by a thick and rounded interzygapophyseal ridge. Small to medium-sized foramina are present on the right lateral surface of the centrum ventral to interzygapophyseal ridge, whereas the left lateral surface bears a series of anteroposteriorly aligned large fossae (Fig. 10.5–10.9). Some of the fossae are pierced by a foramen.

https://doi.org/10.1017/jpa.2025.10101 Published online by Cambridge University Press

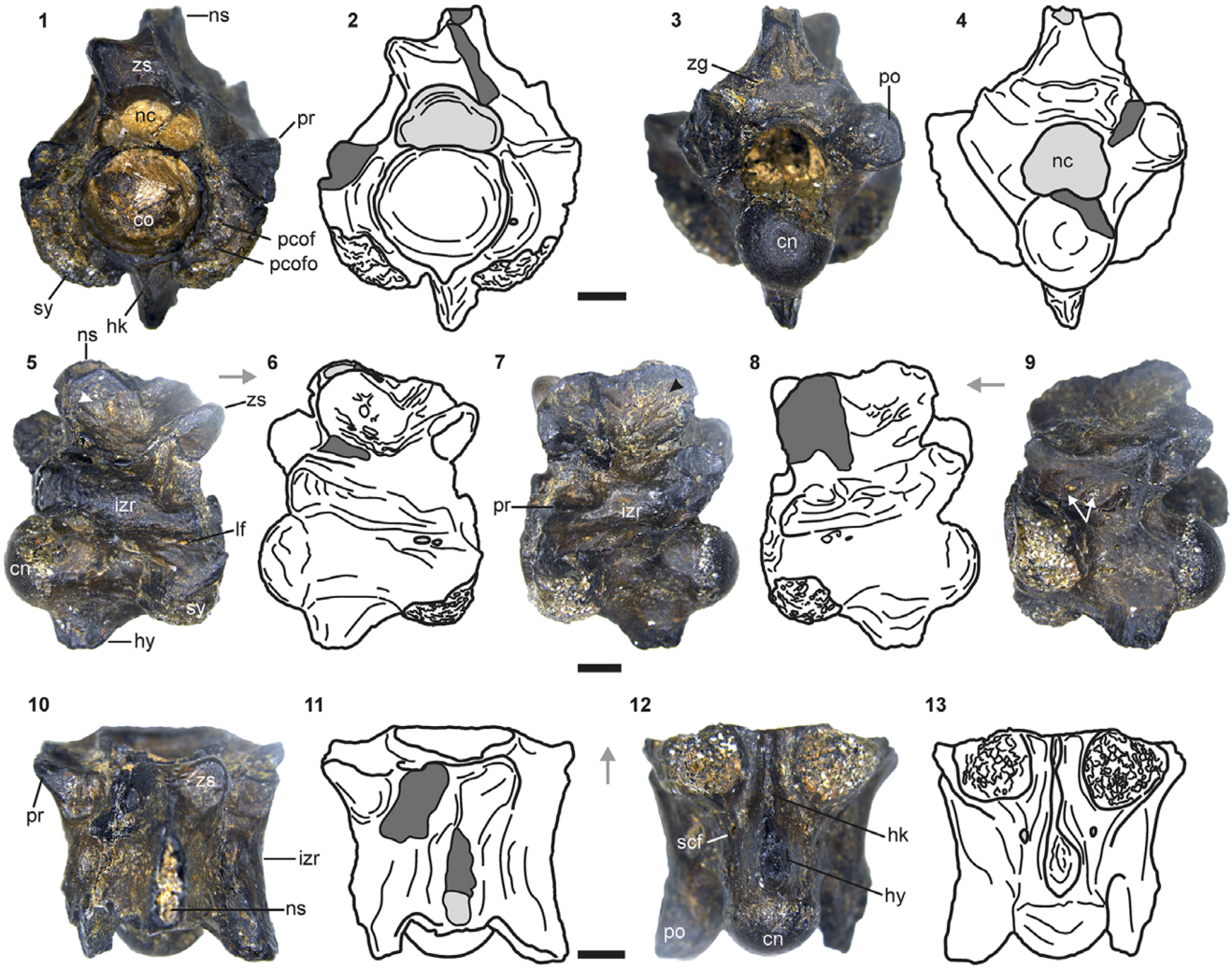

Figure 10. ?Nigerophiidae gen. indet. sp. indet., IITR/VPL/SB 97, nearly complete anterior trunk vertebra shown by actual photographs and interpretative line drawings (in successive order): (**1, 2**) anterior; (**3, 4**) posterior; (**5, 6**) right lateral; (**7, 8**) left lateral; (**9**) left ventrolateral; (**10, 11**) dorsal; and (**12, 13**) ventral views. White arrows and black/white arrowheads indicate anteroposteriorly oriented fossae on lateral surface of centrum and ornamentation of neural arch, respectively. Gray arrows indicate anterior direction. co = cotyle; cn = condyle; hk = hemal keel; hy = hypapophysis; lf = lateral foramen; izr = interzygapophyseal ridge; nc = neural canal; ns = neural spine; pcof = paracotylar foramen; pcofo = paracotylar fossa; po = postzygapophysis; pr = prezygapophysis; scf = subcentral foramen; sy = synapophysis; zg = zygantrum; zs = zygosphene. Scale bars = 2 mm.

Both the neural canal and zygosphene are trilobate/spade-shaped in anterior view, with the canal being slightly narrower than the cotyle (NCW/COW = 0.9; Fig. 10.1, 10.2). The dorsal margin of the zygosphene bears a sharp crest along the midline flanked by a lateral trough. It appears that the dorsal zygosphenal margin, when complete, might have had two troughs separated by a crest in anterior view. The zygosphenal facet is subtriangular and inclined at an angle of 63° from the horizontal. The zygantrum is spade-shaped in posterior view and appears partially roofed, although the zygantral roof is not well preserved (Fig. 10.3, 10.4).

The neural spine is dorsoventrally low (~6% of TVH) and tubular, with a sharp lamina extending from its anterior margin to the dorsal zygosphenal roof (Fig. 10.5–10.11). The neural spine is buttressed posteriorly by thin, posterodorsally directed neural-arch laminae, forming a shallow median embayment. Ventral to the neural spine, multiple shallow fossae that are separated by thin ridges ornament the lateral surface of the neural arch (Fig. 10.5–10.9).

The centrum is triangular in ventral view and slightly narrower posteriorly (Fig. 10.12, 10.13). It bears a sharp hemal keel that gives way posteriorly to a dorsoventrally high hypapophysis. The latter is trapezoidal in lateral view and does not extend to the posterior condyle. A subcentral foramen is present posteromedial to each synapophysis.

Material. IITR/VPL/SB 97, a nearly complete precloacal vertebra.

Remarks. IITR/VPL/SB 97 presents a taxonomic conundrum because many of the features characterizing this snake are commonly found in the aquatic groups Palaeophiidae and Nigerophiidae. Some of these features include laterally flattened vertebra, ventrally deflected synapophysis, reduced prezygapophysis, and cotyle and condyle aligned on a horizontal axis (sensu Rage et al., 2003; Houssaye et al., 2013). Compared with Palaeophiinae, IITR/VPL/SB 97 can be distinguished from *Pterosphenus* based on a trilobate/spade-shaped zygosphene and a neural spine that is separated from the dorsal zygosphenal roof. Furthermore, the lack of a prominent or reduced (knob-like) anterior hypapaophysis differentiates IITR/VPL/SB 97 from ATV and MTV of all *Palaeophis*

https://doi.org/10.1017/jpa.2025.10101 Published online by Cambridge University Press

species. It must be noted, however, that a single (posterior) hypapophysis characterizes *Palaeophis* PTV, although some morphological differences do exist between *Palaeophis* PTV and IITR/VPL/SB 97. In many *Palaeophis* species, the PTV are characterized by ovoid cotyles (e.g., *Palaeophis maghrebianus* [OCP DEK/ GE 517, COW/COH = 1.4], *Palaeophis africanus* [RMCA-RGP 16028a, COW/COH = 1.4], *Palaeophis casei* [COW/COH = 1.4]) and a hypapophysis that is small or even reduced to a hemal keel (Holman, 1982; Houssaye et al., 2013; Folie et al., 2021; Garberoglio et al., 2024). This contrasts with the subcircular cotyle (COW/COH = 1.1) and large hypapophysis seen in IITR/VPL/SB 97. Archaeophiinae, which includes only two known species, *Archaeophis proavus* and '*Archaeophis*' *turkmenicus*, can be distinguished from IITR/VPL/SB 97 by the presence of more elongated vertebrae with synapophyses that remain dorsal to the ventral surface of the centrum and the replacement of hypapophysis by hemal keel in PTV and perhaps also in MTV (Janensch, 1906; Tatarinov, 1963; Rage, 1984; Rage et al., 2003).

On the other hand, IITR/VPL/SB 97 shows a combination of features present in Nigerophiidae (e.g., *Nigerophis mirus*, *Kelyophis hechti*, *Indophis fanambinana*, *I. sahnii*), such as the vertebra being dorsoventrally deeper posteriorly than anteriorly, centrum narrowing posteriorly in ventral view, ventrolaterally positioned synapophyses, low, tubercular neural spine, and a weak median embayment of the neural arch (sensu Rage, 1975, 1984; Rage and Prasad, 1992; LaDuke et al., 2010; Pritchard et al., 2014). Another feature that could further support the possible attribution of IITR/VPL/SB 97 to Nigerophiidae as opposed to Palaeophiidae, is the absence of a pterapophysis based on comparison with the corresponding regions in known nigerophiids and palaeophiids (Fig. 11). Although the neural arch laminae are partially preserved in IITR/VPL/SB 97, the left lamina is strongly ventrolaterally directed and missing only a small portion dorsal to the postzygapophysis. On the other hand, the vertebral dimensions of IITR/VPL/SB 97 are significantly larger than those of any known nigerophiid, and the anterior extent of the neural spine is reminiscent of the condition in palaeophiids. If IITR/VPL/SB 97 is indeed a nigerophid, it represents an ATV as suggested by the presence of a single posterior hypapophysis (sensu Rage, 1984). Limited material currently precludes secure referral of this specimen.

Phylogenetic analysis

Taxa. We only tested the phylogenetic position of *Pterosphenus rannensis* n. sp. and *Pterosphenus biswasi* because they are known from multiple specimens representing the precloacal region whereas the other taxa described in this study are represented by single vertebrae. A modified version of the dataset from Snetkov (2011) was used in the present analysis and comprises 15 taxa including four 'primitive'-grade *Palaeophis* (i.e., *Palaeophis colossaeus*, *Palaeophis africanus*, *Palaeophis maghrebianus*, and *Palaeophis vastaniensis*) and three 'advanced'-grade *Palaeophis* (i.e., *Palaeophis toliapicus*, *Palaeophis typhaeus*, *Palaeophis nessovi*) species along with *Palaeophis oweni*, and five species of *Pterosphenus* (i.e., *Pterosphenus schucherti*, *Pterosphenus schweinfurthi*, *Pterosphenus kutchensis*, *Pterosphenus biswasi*, and *Pterosphenus muruntau*). The basal ophidian *Dinilysia patagonica* Smith-Woodward, 1901 was used as the outgroup. Sources of information are as follows: *D. patagonica* (see Caldwell and Albino, 2003; Scanferla and Canale, 2007), *Palaeophis colossaeus* (Rage, 1983a; Snetkov, 2011; McCartney et al., 2018; Georgalis et al., 2021a), *Palaeophis maghrebianus* (Snetkov, 2011; Houssaye et al., 2013; Georgalis et al., 2021a), and *Palaeophis vastaniensis* (Bajpai and Head, 2007; Snetkov, 2011); *Palaeophis toliapicus* (Owen, 1841; Rage, 1983b; Snetkov, 2011; Zvonok and Snetkov, 2012), *Palaeophis typhaeus* (Owen, 1850; Rage, 1983b); *Palaeophis oweni* (Georgalis et al., 2020); *Palaeophis africanus* (Folie et al., 2021; Georgalis et al., 2021a), *Palaeophis nessovi* (Snetkov, 2011), *Pterosphenus schucherti* (Holman, 1977; Snetkov, 2011; Calvert et al., 2022), *Pterosphenus schweinfurthi* (Snetkov, 2011; McCartney and Seiffert, 2016; Georgalis, 2023), *Pterosphenus kutchensis* (Rage et al., 2003; Snetkov, 2011), *Pterosphenus biswasi* (Rage et al., 2003; Snetkov, 2011), and *Pterosphenus muruntau* (Averianov, 2023).

Characters. The analysis was based exclusively on vertebral characters because knowledge of the palaeophiine skull is nonexistent (Folie et al., 2021). We emphasize that although snake vertebrae are highly useful for taxonomic identification, phylogenetic considerations based on them should be treated with caution because snake vertebrae are strongly influenced by convergence in which many features are repeatedly and independently acquired across diverse lineages (Smith and Georgalis, 2022; Szyndlar and Georgalis, 2023). The phylogenetic analysis presented here is subject to possible uncertainties arising from our limited understanding of intracolumnar variation in palaeophiines (Houssaye et al., 2013; Folie et al., 2021) and should therefore be treated with caution. We still tested the phylogenetic position of *Pterosphenus rannensis* n. sp. (considering its intermediate morphology between *Palaeophis* and *Pterosphenus*) and that of *Pterosphenus biswasi* in view of the concerns raised about its validity. Thirty vertebral characters (Appendix 3) were used of which 26 were from Snetkov (2011). Four of these characters were modified (characters [chs.] 1, 11, 12, 14) and four new characters were added (chs. 27–30). Furthermore, to have at least twice the number of characters than species analyzed (sensu Hammer and Harper, 2006; Folie et al., 2021), the analysis included only 15 taxa.

Results. The character-taxon matrix comprising 15 taxa and 30 characters (Supplementary Dataset 1) was analyzed using TNT version 1.6 (Goloboff and Morales, 2023) with the software memory set to retain 10,000 trees and a display buffer of 10 Mb. The Traditional Search option was used in which the analysis constraints included 50 replications of Wagner trees, with bisection reconnection as the swapping algorithm, and 10 trees saved per replication. Robustness of nodes was determined from (1) Bremer support values, calculated using script bremer.run in which only trees suboptimal by 20 steps were retained, and (2) symmetric resampling values based on 1,000 replicates and expressed as frequency differences. Three most parsimonious trees (MPTs; Fig. 12.1, 12.2) were recovered with a tree length of 69, consistency index (CI) of 0.449, and retention index (RI) of 0.6. In both the strict and majority-rule trees, *Pterosphenus* was well resolved and a later-diverging relative to all *Palaeophis* snakes. Within *Pterosphenus*, *Pterosphenus rannensis* n. sp. was the earliest-diverging taxon followed by *Pterosphenus biswasi*, whereas *Pterosphenus schucherti* and *Pterosphenus schweinfurthi* constituted the latest-diverging subclade. Four unambiguous synapomorphies support the recovery of *Pterosphenus rannensis* n. sp. as the basalmost *Pterosphenus*: zygosphene with dorsoventrally high midline crest (ch. 1), thick zygosphene (ch. 2), anterior margin of neural spine extends to the dorsal zygosphenal roof (ch. 14), and distance between prezygapophysis less than the distance measured from the ventral cotylar rim to the dorsal zygosphenal margin (ch. 22). Furthermore, two local autapomorphies diagnose *Pterosphenus rannensis* n. sp.: absence of subcentral foramina (ch. 15) and pterapophysis remaining below the dorsal zygosphenal margin (ch. 28).

https://doi.org/10.1017/jpa.2025.10101 Published online by Cambridge University Press

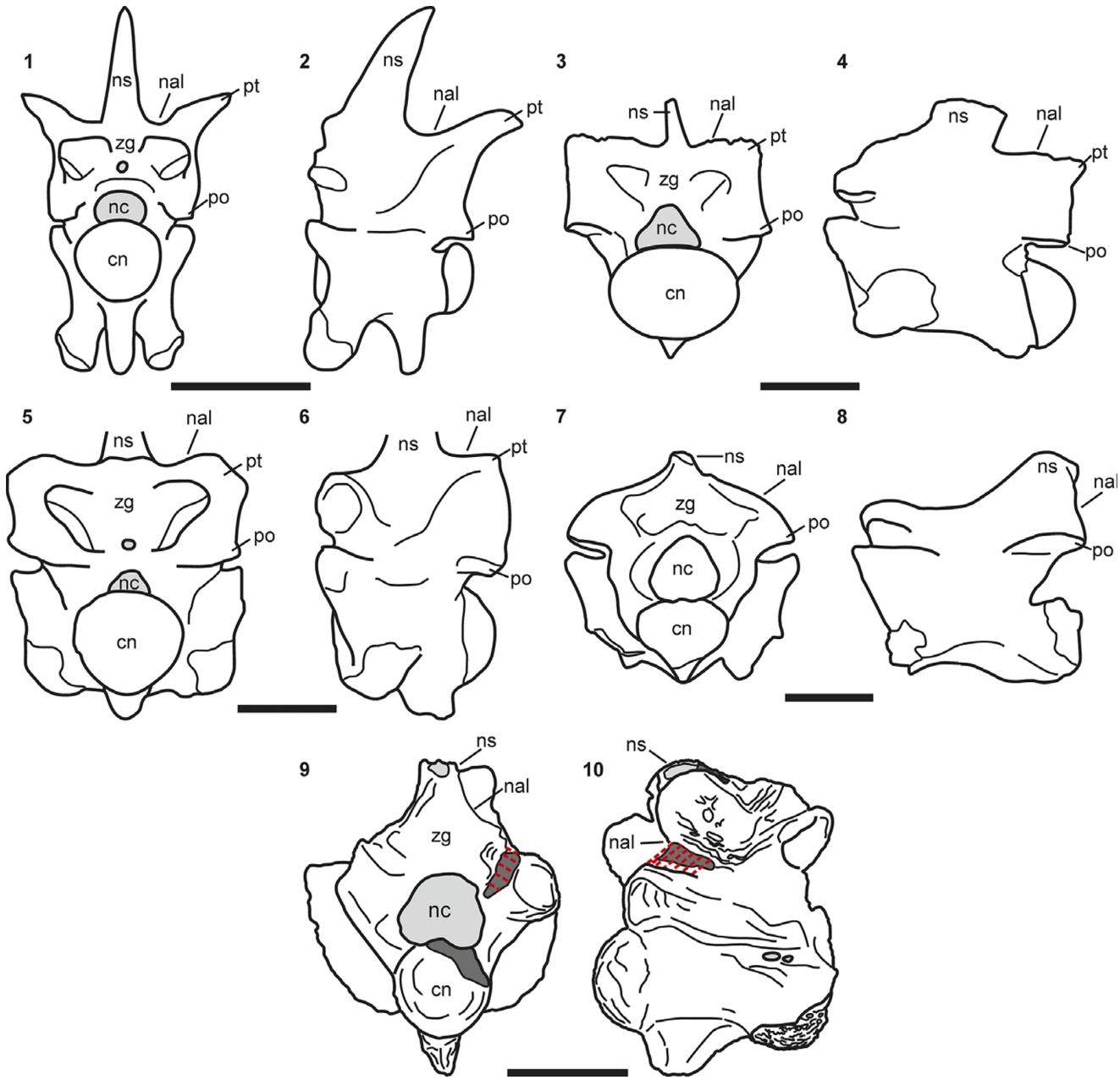

Figure 11. Comparison of IITR/VPL/SB 97 (?Nigerophiidae gen. indet. sp. indet.) with precloacal vertebrae of other nigerophiids and palaeophiids: (**1, 2**) *Pterosphenus kutchensis* Rage et al., 2003; (**3, 4**) *Palaeophis nessovi* Averianov, 1997; (**5, 6**) *Palaeophis colossaeus* Rage, 1983a; (**7, 8**) *Indophis sahnii* Rage and Prasad, 1992; and (**9, 10**) IITR/VPL/SB 97 (red dashed lines indicate missing areas of neural arch laminae dorsal to postzygapophysis): (**1, 3, 5, 7, 9**) posterior; (**2, 4, 6, 8**) left lateral; and (**10**) right lateral views. Schematic diagrams based on the following sources: (**1, 2**) RUSB 2721-1 (holotype), RUSB 2790-1 (Rage et al., 2003; Garberoglio et al., 2024); (**3, 4**) ZIN PH 119/1 (Snetkov, 2011); (**5, 6**) MNHN.F. TGE615 (holotype; Rage, 1983a; Garberoglio et al., 2024); (**7, 8**) VPL/JU/500 (holotype; Rage and Prasad, 1992). cn = condyle; nal = neural arch lamina; nc = neural canal; ns = neural spine; po = postzygapophysis; pt = pterapophysis; zg = zygantrum. Scale bars = 2 mm.

Unlike *Pterosphenus*, a fully resolved picture of *Palaeophis* interrelationships is only seen in the majority-rule tree (Fig. 12.2). Here, *Palaeophis vastaniensis* is the basalmost palaeophiine with the other 'primitive'-grade paleophiids (*Palaeophis maghrebianus* and *Palaeophis africanus*) also restricted to the basal part of the tree. An exception to this is *Palaeophis colossaeus*, which, together with the 'advanced'-grade *Palaeophis toliapicus*, constituted the latest-diverging clade of *Palaeophis* closest to *Pterosphenus*. As for the other 'advanced'-grade palaeophiids, *Palaeophis typhaeus* was a sister taxon to *Palaeophis oweni*, whereas *Palaeophis nessovi* was recovered in a more basal position, being phylogenetically bracketed by *Palaeophis maghrebianus* and *Palaeophis africanus*.

Discussion. The in-group relationships of Palaeophiinae obtained here failed to recover a monophyletic *Palaeophis*, consistent with the results of Snetkov (2011) and Folie et al. (2021). Rather, the *Palaeophis* species formed successive outgroups to *Pterosphenus*, on which the earliest branching were, mostly, the 'primitive'-grade *Palaeophis* taxa, followed by the 'advanced'-grade forms (Fig. 12.1, 12.2). Such an arrangement of taxa essentially mirrors the three

https://doi.org/10.1017/jpa.2025.10101 Published online by Cambridge University Press

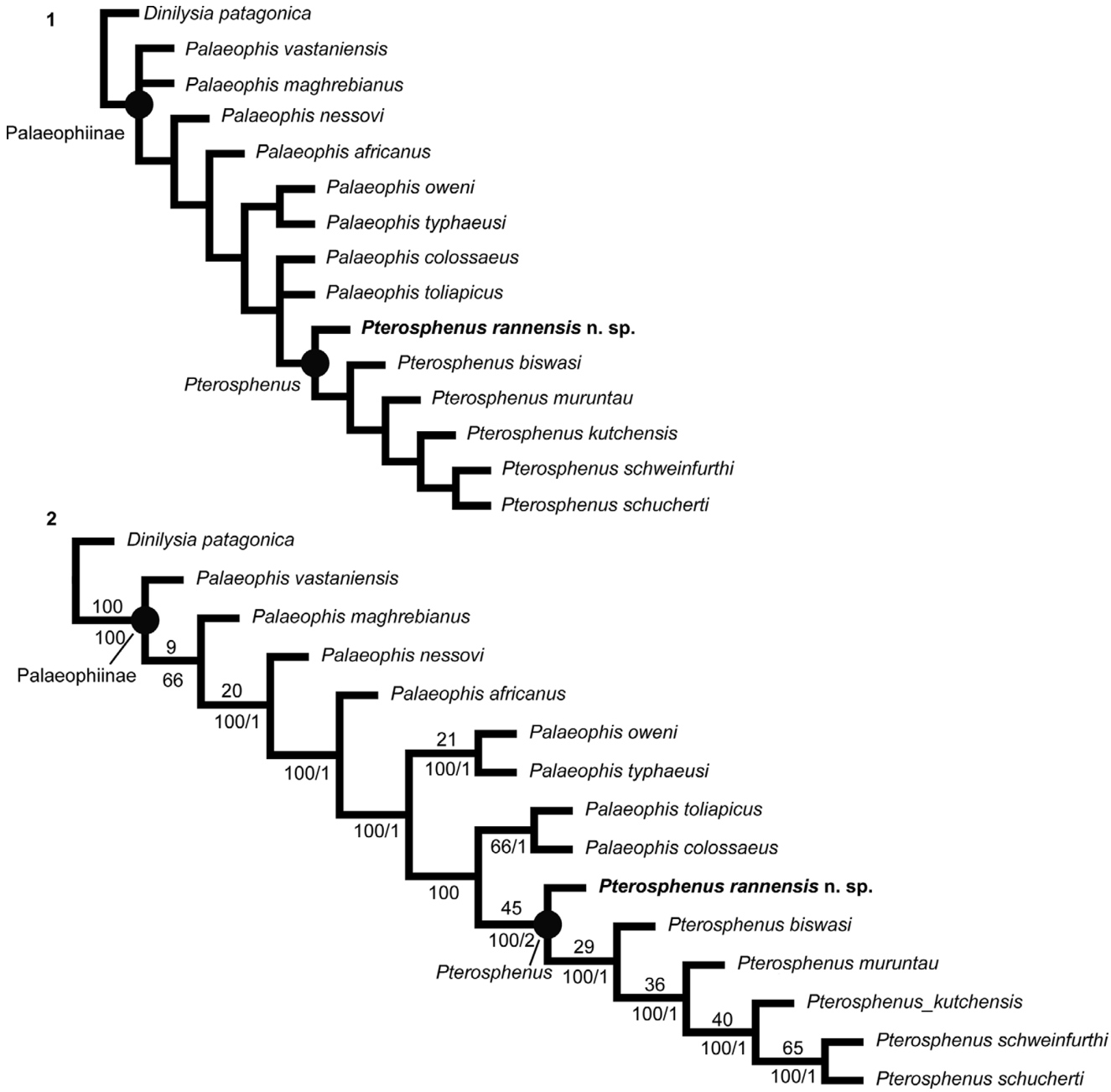

Figure 12. (**1**) Strict consensus tree of three MPTs showing palaeophiinae inter-relationships, and (**2**) 50% majority-rule tree showing inter-relationships of palaeophiine snakes; *Pterosphenus rannensis* n. sp. given in bold. Numbers below nodes indicate the frequency that a clade is represented in the MPTs (left) and Bremer support values (right). Numbers above nodes indicate group present/contradicted (GC) symmetric resampling values.

ecological grades identified within Palaeophiinae (sensu Rage et al., 2003) because it presents a morphological series ranging from snakes that are poorly adapted to aquatic life to those that are strongly adapted. Some of the major evolutionary trends defining this series are consistent with the morphological changes associated with the ecological grades by Rage et al. (2003) and include progressive thickening of the zygosphene and development of a dorsoventrally high central crest on the dorsal zygosphenal surface (chs. 1, 2), increase in the ventral extent of the synapophyses (ch. 11), increased lateral flattening of vertebrae (ch. 12), anterior margin of the neural spine extending to the zygosphene (ch. 14), progressive increase in height of the pterapophysis relative to the dorsal margin of zygosphene and the length of the centrum (chs. 28, 29), and development of a marked concavity along the pterapophysis-postzygapophysis connection (ch. 30). The only taxon that diverges from this morphological series is *Palaeophis colossaeus*, which has a sister-taxon relationship with the 'advanced'-grade *Palaeophis toliapicus* despite being identified as a 'primitive'-grade form (sensu Rage et al., 2003). A possible explanation for this could be the presence of some shared features between *Palaeophis colossaeus* and *Palaeophis toliapicus*, e.g., a thick zygosphene (ch. 2), a weak interzygapophyseal ridge (ch. 6), angle formed by V-shaped incision on the posterior part of the neural arch > 105° (ch. 25), and the pterapophysis extending slightly above the zygosphene (ch. 28).

The *Pterosphenus* in-group relationships obtained here corroborate our taxonomic inferences concerning *Pterosphenus rannensis*

https://doi.org/10.1017/jpa.2025.10101 Published online by Cambridge University Press

n. sp. and *Pterosphenus biswasi*. The new taxon *Pterosphenus rannensis* n. sp. presents a host of morphological features that characterize both *Palaeophis* [e.g., shallow ventral extent of the synapophyses (ch. 11); weak lateral flattening of the vertebrae (ch. 12); pterapophysis-postzygapophysis connection lacking a marked concavity (ch. 30)] and *Pterosphenus* (e.g., dorsoventrally high central crest on the dorsal surface of the zygosphene [ch. 1]; anterior margin of the neural spine extending to the zygosphene [ch. 14]). This reflects the intermediate phylogenetic position of this taxon relative to *Pterosphenus* and *Palaeophis* and supports our osteological study, which highlighted the intermediate morphology of *Pterosphenus rannensis* n. sp. The anatomical and phylogenetic position of *Pterosphenus rannensis* n. sp. and African *Pterosphenus* of similar nature (see Zouhri et al., 2018) hint at the possibility of the distinction between *Pterosphenus* and *Palaeophis* being artificial and highlights the need for a revision of the subfamily Palaeophiinae, as suggested by Rage et al. (2003) and Smith and Georgalis (2022). The early-diverging position of *Pterosphenus biswasi*, distinct from *Pterosphenus schucherti* and *Pterosphenus schweinfurthi*, supports its validity. Its distinctiveness from *Pterosphenus schucherti* and *Pterosphenus schweinfurthi* was supported by a combination of features, including a prominent interzygapophyseal ridge (ch. 6), weak lateral compression of vertebrae (ch. 12), centrum length less than the distance between the lateral margin of synapophyses (ch.13), pterapophysis extending slightly above the zygosphene (ch. 28), PTH/CL < 0.7 (ch. 29), and pterapophysis-postzygapophysis connection without marked concavity (ch 30). It should be noted that Snetkov (2011) in his phylogenetic analysis of Palaeophiidae also recovered *Pterosphenus biswasi* as distinct from *Pterosphenus schucherti* and *Pterosphenus schweinfurthi.*

Significance of the fauna

Paleobiogeogrpahy and paleoecology. Fossil snakes from the Eocene of Kutch described herein represent a varied fauna that has elements that are both cosmopolitan and predominantly Gondwanan in nature. The madtsoiid (IITR/VPL/SB 2782) and possible nigerophiid (IITR/VPL/SB 97) from the Naredi Formation represent Gondwanan elements because these ophidian families are largely known from Gondwanan landmasses (Rage and Prasad, 1992; LaSuke et al., 2010; Rio and Mannion, 2017; Datta and Bajpai, 2024). The cosmopolitan elements of this fauna are represented by the palaeophiines, *Pterosphenus rannensis* n. sp., and IITR/VPL/SB 2632 from the stratigraphically younger Harudi Formation.

Palaeophiinae. The presence of palaeophiine fossils in Eocene deposits is not unexpected considering their prolific diversification during this period (McCartney and Seiffert, 2016; Folie et al., 2021; Smith and Georgalis, 2022; Garberoglio et al., 2024). The oldest record of Palaeophiinae comes from the Late Cretaceous of Africa, followed by their restricted occurrence in the Paleocene (Rage and Wouters, 1979; Erickson, 1998; Garberoglio et al., 2024). These snakes became truly cosmopolitan only during the Eocene, with reports from Africa, the Americas, Asia, Europe, and India (Rage, 1983b; Rage et al., 2003, 2008; Folie et al., 2021; Georgalis et al., 2021a; Smith and Georgalis, 2022). Among the two phenotypic genera nested within this subfamily (sensu Rage et al., 2003), the *Palaeophis*-type snakes show a wider temporal range extending from the Late Cretaceous to the late Eocene (Rage et al., 2008; Head et al., 2022; Smith and Georgalis, 2022). *Pterosphenus*-type snakes, on the other hand, are restricted to the Eocene, with most taxa reported from horizons that are either early Lutetian or Bartonian-Priabonian in age (Rage et al., 2008; Folie et al., 2021; Smith and Georgalis, 2022; Georgalis, 2023; Datta and Bajpai, 2024, supplementary note 1). There appear to be no known Ypresian and middle/late Lutetian occurrences globally, possibly as a result of sampling bias, except for an isolated vertebra from the Cambay Shale Formation of India, which is the only record of this genus from the Ypresian (Rage et al., 2008). The late Lutetian palaeophiine taxa described here (*Pterosphenus rannensis* n. sp. and ? *Palaeophis* sp.), along with the recently described remains of *Pterosphenus schucherti* from Kutch (Natarajan et al., 2024), bridge this temporal gap. These taxa also represent stratigraphically the youngest record of Palaeophiidae in the Indian subcontinent. The phylogenetic position of *Pterosphenus rannensis* n. sp. presents some interesting biogeographic scenarios. The basal position of *Pterosphenus rannensis* n. sp. relative to the other Indian *Pterosphenus*-grade snakes (*Pterosphenus biswasi*, *Pterosphenus kutchensis*) needs to be reconciled in view of the younger age of *Pterosphenus rannensis* n. sp. The latter taxon appears to be the relic of a long-surviving, early-diverging lineage that gave rise to the more-derived *Pterosphenus biswasi* and *Pterosphenus kutchensis.* Moreover, the phylogenetic placement of *Pterosphenus rannensis* n. sp. also highlights the significance of the Indian record to understanding the origin and diversification of the genus, mainly due to the intermediate morphology of *Pterosphenus rannensis* n. sp., which is reminiscent of both *Palaeophis* and *Pterosphenus.* In this scenario, the Ypresian *Pterosphenus* sp. indet. (GU/RSR/VAS 1009) from the Cambay Shale Formation becomes important because it represents the earliest global record of this genus (Rage et al., 2008) although its poor preservation does not allow for specific identification at present. Alternatively, a dispersal event from Africa to explain the occurrence of *Pterosphenus rannensis* n. sp. cannot be ruled out considering the marine adaptations of palaeophiine snakes and the recovery of the oldest (Late Cretaceous) member of this subfamily (*Palaeophis* sp.) from that continent. Faunal exchanges between Africa and the Indian subcontinent during the Paleogene have been previously suggested for a diverse array of aquatic taxa including pelomedusoid turtles, dyrosaurid crocodyliforms, and madtsoiid and colubroid snakes (Smith et al., 2016; Zaher et al., 2021; Datta and Bajpai, 2024). Instances of an African-North American transoceanic dispersal has been observed in *Palaeophis africanus* and *Pterosphenus schweinfurthi* (Andrews, 1924; Parmley and DeVore, 2005; McCartney and Seiffert, 2016; Georgalis et al., 2021a; Smith and Georgalis, 2022; Georgalis, 2023). A similar dispersal event from India, across marine waters, could also explain the phylogenetic position of the Asian *Pterosphenus muruntau* (Bartonian; Averianov, 1997, 2023), which is phylogenetically bracketed by the stratigraphically older *Pterosphenus biswasi* and *Pterosphenus kutchensis.* Nonetheless, the biogeographic scenarios presented here should be treated as tentative considering that the present phylogenetic results are based solely on vertebrae. We also stress the need for more extended collection efforts in the Cretaceous and Palaeogene deposits across the globe because it could lead to recovery of more phylogenetically informative material allowing a better understanding of Palaeophiinae biogeography.

An aquatic habitus is typically inferred for palaeophiine snakes based on vertebral morphology and because their fossil remains have been recovered from various aquatic environments ranging from lagoons, estuaries, mangrove forests, and near-coastal fluvial to shallow/nearshore marine settings (Hoffstetter, 1958; Westgate and Ward, 1981; Holman, 1982; Rage, 1983a; Hutchison, 1985; Westgate and Gee, 1990; Rage et al., 2003; Parmley and DeVore, 2005; Houssaye et al., 2013; McCartney et al., 2018; Folie et al., 2021;

https://doi.org/10.1017/jpa.2025.10101 Published online by Cambridge University Press

Georgalis et al., 2021a). However, based on the degree of development of vertebral features associated with aquatic adaptations (e.g., laterally compressed vertebrae, ventrally shifted synapophyses with facets facing ventrally to place the ribs beneath the vertebrae, and the presence of pterapophyses), *Pterosphenus* snakes are considered better adapted to this mode of life than *Palaeophis*-grade snakes. Accordingly, the latter taxa are considered as nonpelagic, whereas remains of *Pterosphenus* have been reported from an open marine environment (Westgate, 2001; Rage et al., 2003; Houssaye et al., 2013).

From a paleoecological standpoint, the two palaeophiines described here, *Pterosphenus rannensis* n. sp. and ?*Palaeophis* sp. (IITR/VPL/SB 2632), together with the recently described *Pterosphenus schucherti* by Natarajan et al. (2024), present an ecological conundrum. All three taxa are from the Harudi Formation, albeit from different localities, and present a scenario rarely seen among palaeophiines. The co-occurrence of *Palaeophis* and *Pterosphenus* in the same stratigraphic context is known only from the early Eocene Cambay Shale Formation of India, and the late Eocene of the Hardie Mine in the USA (Parmley and DeVore, 2005; Rage et al., 2008). Ecological segregation/niche partitioning seems to be a likely explanation for this conundrum in view of the hypothesized differences in aquatic adaptaions between *Pterosphenus* and *Palaeophis* (Westgate, 2001; Rage et al., 2003; Houssaye et al., 2013). Natarajan et al. (2024) considered a marginal marine habitat for *Pterosphenus schucherti* based on nearshore bivalves, gastropods, and nautiloids from the fossil locality at Rato River (the type section of the Harudi Formation). *Pterosphenus schucherti* is generally considered to have lived in coastal to shallow shelf waters, similar to the extant yellow-bellied sea snake, and sporadically moved into the open ocean (Hecht et al., 1974; Natarajan et al., 2024). As for *Pterosphenus rannensis* n. sp. and ?*Palaeophis* sp., the inferred depositional setting of the fossil localities indicates contrasting habitats. Based on sedimentology, tidal and lagoonal lithofacies (Mukhopadhyay and Shome, 1996; Thewissen and Bajpai, 2009) were suggested for the Godhatad and Dhedidi North localites from which came the fossils of *Pterosphenus rannensis* n. sp. Evidence for the depositional conditions also comes from the associated fauna of fossil whales (Thewissen and Bajpai, 2009) and mollusks including oysters (Banerjee et al., 2019). Protocetids, which occur abundantly at the *Pterosphenus rannensis* n. sp.-yielding beds at Godhatad and Dhedidi North, support a tidal to shallow coastal marine environment (Thewissen and Bajpai, 2009; Thewissen et al., 2009; Bajpai and Thewissen, 2014). Regarding ?*Palaeophis* sp., a marshy/swampy environment was proposed for the Babia Hill locality (Mukhopadhyay and Shome, 1996). The abundance of remingtonocetines and near absence of protocetids at this locality corroborate the inferred paleoenviroment, because the small orbits in *Remingtonocetus* Kumar and Sahni, 1986 have been considered an adaptation to the muddy waters expected in a swamp/marsh (Thewissen and Bajpai, 2009; Bajpai et al., 2011). The rarity of ?*Palaeophis* (single vertebra) at this locality, however, might suggest that this specimen was transported.

Interestingly, the vertebral morphology of the two new Harudi palaeophiines is not consistent with their inferred paleohabitats. The vertebrae of *Pterosphenus rannensis* n. sp. do not show strong near-shore aquatic adaptations commonly associated with *Pterosphenus*, e.g., strongly laterally compressed vertebrae with high pterapophyses (sensu Rage et al., 2003). ?*Palaeophis* sp., which possibly lived in a swamp/marsh, shows pronounced aquatic adaptations, e.g., strong lateral vertebral compression and a high pterapophysis (see McCartney et al., 2018). Another example reminiscent of *Pterosphenus rannensis* n. sp. is *Palaeophis colossaeus*, which comes from a nearshore marine environment, although this snake is not considered to have strong adaptations to aquatic life (Rage, 1983a; McCartney et al., 2018). Our study thus highlights the need for re-evaluation of morphological correlates of aquatic adaptations in fossil snakes. Although the present observations seemingly support the presence of niche partitioning among the two Harudi palaeophiines described here, we still consider this inference tentative and subject to confirmation from additional material. We recognize that the burial site of fossils, which in our case includes disarticulated/isolated vertebrae, does not always coincide with the habitat area. Nonetheless, the Kutch specimens of *Pterosphenus rannensis* n. sp. do not appear to have suffered long transportation because they are not strongly abraded or deformed, as evident from the high angularity and low sphericity of the specimens (see Mukherjee and Ray, 2012; Datta et al., 2020).

Madtsoiidae. IITR/VPL/SB 2782 potentially enriches the known diversity of Indian madtsoiids, the temporal range of which extends from the latest Cretaceous to the late Oligocene (Rage et al., 2004; Mohabey et al., 2011; Smith et al., 2016; Wazir et al., 2021; Head et al., 2022; Smith and Georgalis, 2022; Datta and Bajpai, 2024). Although an isolated vertebra does not allow a confident generic or specific designation, the morphological similarities and differences of IITR/VPL/SB 2782 with the contemporaneous (early Lutetian) *Vasuki indicus* highlight the uniqueness of this taxon. It is likely that IITR/VPL/SB 2782 and *Vasuki* belong to the same lineage. Datta and Bajpai (2024) argued for an Indian origin of the madtsoiid lineage leading to *Vasuki*, and we think that IITR/VPL/SB 2782 provides further evidence for the evolutionary diversification of this lineage. The vertebral morphology of IITR/VPL/SB 2782 also allows for paleoecological interpretations. An ecological habitus similar to that of *Vasuki* (back-swamp marsh; Datta and Bajpai, 2024) is envisaged for IITR/VPL/SB 2782 based on their shared morphology, consistent with previous paleoenvironmental interpretations based on sedimentological data (Mukhopadhyay and Shome, 1996) and associated vertebrates (abundant mylobatids, catfishes, sharks, crocodilians, trionychid turtles, and archaic whales) (Bajpai and Thewissen, 2002). IITR/VPL/SB 2782 was a large, slow-moving snake with a cylindrical body, given that the vertebra is longitudinally short and transversely wide, with laterally facing synapophyses that would have supported laterally directed ribs (sensu Mosauer, 1932; LaDuke et al., 2010; McCartney et al., 2018; Datta and Bajpai, 2024). These features argue against an aquatic lifestyle for IITR/VPL/SB 2782 (Rage et al., 2003; Houssaye et al., 2013; McCartney et al., 2018; Georgalis, 2023). We, however, cannot completely rule out an aquatic lifestyle for IITR/VPL/SB 2782 because some features associated with aquatic adaptations show inconsistencies in some aquatic snakes. For example, true lateral vertebral compression is only seen in the caudal region of hydrophiine sea snakes, whereas in the Cretaceous aquatic snake *Simoliophis* Sauvage, 1880, the synapophyses shift from ventrally to laterally facing across the vertebral column (Rage et al., 2016; Datta and Bajpai, 2024). An arboreal or fossorial lifestyle also seems unlikely for IITR/VPL/SB 2782 because of its large size, obliquely directed prezygapophyseal articular facets in dorsal view, and a broad hemal keel (see Szyndlar and Georgalis, 2023). Furthermore, the vertebrae of arboreal snakes are often longer and have shorter zygapophyses, whereas fossorial snakes tend to have depressed neural arch-spine complexes that place the epaxial muscles close to the sagittal plane (Johnson, 1955; Auffenberg, 1961; LaDuke et al., 2010). Therefore, a terrestrial/semiaquatic mode of life is more likely for IITR/VPL/SB 2782, as previously suggested for

https://doi.org/10.1017/jpa.2025.10101 Published online by Cambridge University Press

Vasuki indicus (sensu Datta and Bajpai, 2024). Moreover, like the latter taxon, this snake would have been an ambush predator that subdued prey by constriction.

Nigerophiidae. IITR/VPL/SB 97 is tentatively assigned to Nigerophiidae and is among the oldest fossil snakes from the Paleogene of India (Ypresian). If this assignment is accurate, then this specimen represents one of the oldest Cenozoic records of Nigerophiidae globally, and possibly the first record of this family from the Cenozoic of South Asia. Unfortunately, given its tentative taxonomic status, IITR/VPL/SB 97 does not provide reliable insights into the biogeography of Nigerophiidae. The same can also be said for other known Late Cretaceous/Paleogene nigerophiids because of the uncertainties surrounding the monophyly of this family and its in-group relations (LaDuke et al., 2010; Pritchard et al., 2014). However, the discovery of the Indian nigerophiid *Indophis* Rage and Prasad, 1992 from the Late Cretaceous of Madagascar has led some authors to propose Indo-Madagascar biotic links during this geological interval (Pritchard et al., 2014; Rage et al., 2020). Paleoecologically, nigerophiids have traditionally been regarded as aquatic snakes based on vertebral morphology (e.g., ventrally shifted synapophyses, narrow prezygapophyseal buttress with anterolateral convexity and high vertebrae), with fossils recovered from freshwater lacustrine to marginal/shallow marine deposits (Rage and Prasad, 1992; Prasad and Khajuria, 1996; Rage et al., 2004, 2020; LaDuke et al., 2010; Houssaye et al., 2013; McCartney et al., 2018; Smith and Georgalis, 2022). We also envisage an aquatic lifestyle for IITR/VPL/SB 97 based on the ventrally deflected synapophyses that extend below the centrum, the sharp and anterolaterally convex prezygapophyseal buttress, and the dorsoventral height of the vertebra. Supporting evidence comes from the depositional environment of the horizon yielding IITR/VPL/SB 97, which was reconstructed as a brackish to marine inner shelf based on benthic foraminiferans, bivalves, and fishes including gars (Keller et al., 2013; Khozyem et al., 2013).

Conclusions

A diverse snake fauna, comprising both cosmopolitan taxa and Gondwana holdovers from the Late Cretaceous, is described from the Eocene of Kutch, western India. The Cretaceous relics include a large madtsoiid and a possible nigerophiid, the former being sympatric to the early Lutetian giant madtsoiid *Vasuki indicus*. The nigerophiid, on the other hand, is stratigraphically among the oldest Paleogene snakes known from India. The cosmopolitan elements, represented by late Lutetian palaeophiines, are represented by *Pterosphenus* (*Pterosphenus rannensis* n. sp.) and ? *Palaeophis*, the latter sharing affinities with 'advanced'-grade *Palaeophis*. *Pterosphenus rannensis* n. sp. is characterized by an intermediate vertebral morphology that is reminiscent of both *Pterosphenus* and *Palaeophis*.

Pterosphenus biswasi, originally described by Rage et al. (2003) from the middle Eocene of Kutch and subsequently synonymized with *Pterosphenus schucherti* (Natarajan et al., 2024), is re-examined here. Based on the presence of a low pterapophysis and weak lateral vertebral flattening, we retain *Pterosphenus biswasi* as a valid taxon.

Phylogenetic analysis corroborated our anatomical observations because it recovered *Pterosphenus rannensis* n. sp. and *Pterosphenus biswasi* at the base of the clade comprising all *Pterosphenus* snakes. *Pterosphenus rannensis* n. sp. is the earliest-diverging member of this clade and occupies an intermediate position between *Pterosphenus*- and *Palaeophis*-grade snakes. Furthermore, the biogeography of palaeophiines, seen in conjunction with the phylogenetic position and stratigraphic age of *Pterosphenus rannensis* n. sp., highlights the importance of India as a center for the diversification of *Pterosphenus*.

Based on vertebral morphology, an aquatic habitus is suggested for most taxa in this fauna except for the madtsoiid, which was terrestrial/semiaquatic. Niche partitioning is observed among the two palaeophiine snakes, based on depositional environment of the fossil-yielding horizons.

The present study provides, for the first time, insights into ophidian diversity during the middle Eocene of India, besides augmenting the known diversity of Indian Eocene snakes. When compared with the subcontinent's Late Cretaceous record, the Eocene snake diversity shows marked differences in faunal composition and ecological preferences. The Cretaceous fauna is largely known from terrestrial/freshwater settings and includes stem snakes (*Coniophis* Marsh, 1892; *Sanajeh* Wilson Mantilla et al., 2010), madtsoiids (indeterminate forms; *Madtsoia pisdurensis*), and a nigerophiid (*Indophis sahnii*) (Rage and Prasad, 1992; Rage et al., 2004, 2020; Wilson Mantilla et al., 2010; Mohabey et al., 2011). On the contrary, the Eocene fauna is marked by the appearance of palaeophiids, constrictors, and caenophidians, aside from nigerophiids and madtsoiids that survived from the Cretaceous (Rage et al., 2003, 2008; Smith et al., 2016; Datta and Bajpai, 2024). The paleoecological contexts of these snakes range from aquatic (swamp to marginal marine) to amphibious and terrestrial. The observed faunal turnover was most likely related to the end-Cretaceous extinction event, which extinguished countless terrestrial and marine vertebrates. The niches vacated by the K-Pg extinction allowed snakes to not only occupy these ecological spaces but also to venture into new morphospaces.

Acknowledgments. The authors acknowledge with thanks the helpful comments, suggestions, and a constructive critique of the manuscript by J. Calede (Editor), H.-D. Sues (Associate Editor), J. Kastigar (Managing Editor), G. Georgalis, and an anonymus reviewer. We thank R. Sharma, D. Das, V.V. Kapur, N. Saravanan, L. Cooper, L. Stevens, and H. Thewissen for help during fieldwork and A. Saha and A. Rautela for help and discussions. The Science and Engineering Research Board (now ANRF) (Grant no. PDF/2021/000468 for National Post-doctoral Fellowship to DD), IIT Roorkee for Institute Post Doctoral Fellowship to DD, and the Department of Science and Technology (SB), Government of India are acknowledged for financial support. DD would like to acknowledge IIT Roorkee for providing infrastructural facilities. SB would like to acknowledge support obtained from IIT Roorkee as part of his Institute Chair Professorship.

Competing interests. Authors declare no competing interests.

Data availability statement. All appendices are available from Dryad Digital repository: https://doi.org/10.5061/dryad.z8w9ghxq2. Supplementary data are available from Morphobank (http://morphobank.org/permalink/?P5887).

References

Agrawal, S., Verma, P., Rao, M.R., Garg, R., Kapur, V.V., and Bajpai, S., 2017, Lignite deposits of the Kutch Basin, western India: carbon isotopic and palynological signatures of the early Eocene hyperthermal event ETM2: *Journal of Asian Earth Sciences*, **v. 146**, p. 296–303, https://doi.org/10.1016/j.jseaes.2017.04.030

Andrews, C.W., 1901, Preliminary notes on some recently discovered extinct vertebrates from Egypt (part 2): *Geological Magazine*, **v. 8**, p. 436–444.

Andrews, C.W., 1924, Note on some ophidian vertebrae from Nigeria: *Geological Survey of Nigeria*, **v. 7**, p. 39–43.

Aniny, F., Georgalis, G.L., Gingerich, P.D., and Zouhri, S., 2024, Occurrence of the large aquatic snake *Palaeophis* cf. *africanus* (Serpentes, Palaeophiidae) in the middle Eocene of the Sabkha El Breij, southwestern Morocco: *Historical Biology*, **v. 37**, no. 4, p. 1–6, https://doi.org/10.1080/08912963.2024.2352863

Arambourg, C., 1952, Les vertébrés fossiles des gisements de phosphates (Maroc-Algérie-Tunisie): *Notes et Mémoires du Protectorat de la République Française au Maroc, Direction de la Production Industrielle et des Mines, Division des Mines et de la Géologie, Service Géologique du Maroc*, **v. 92**, p. 1–372.

Auffenberg, W., 1961, Additional remarks on the evolution of trunk musculature in snakes: *American Midland Naturalist*, **v. 65**, p. 1–16.

Averianov, A.O., 1997, Paleogene sea snakes from the eastern part of Tethys: *Russian Journal of Herpetology*, **v. 4**, p. 128–142.

Averianov, A.O., 2023, *Pterosphenus muruntau*—valid species of sea snakes (Squamata: Palaeophiidae) from the middle Eocene of Uzbekistan: *Zoosystematica Rossica*, **v. 32**, p. 85–92, https://doi.org/10.31610/zsr/2023.32.1.85

Bajpai, S., and Head, J.J., 2007, An early Eocene palaeopheid snake from Vastan Lignite Mine, Gujarat, India: *Gondwana Geological Magazine*, **v. 22**, p. 85–90.

Bajpai, S., and Thewissen, J.G.M, 2000, A new diminutive Eocene whale from Kachchh (Gujarat, India) and its implications for locomotor evolution of cetaceans: *Current Science*, **v. 79**, p. 1478–1482.

Bajpai, S., and Thewissen, J.G.M., 2002, Vertebrate fauna from Panandhro lignite field (lower Eocene), District Kachchh, western India: *Current Science*, **v. 82**, p. 507–509.

Bajpai, S. and Thewissen, J.G.M., 2014, Protocetid cetaceans (Mammalia) from the Eocene of India: *Palaeontologia Electronica*, **v. 17**, n. 3.34A, https://doi.org/10.26879/459

Bajpai, S., Thewissen, J.G.M., Kapur, V.V., Tiwari, B.N., and Sahni, A., 2006, Eocene and Oligocene sirenians (Mammalia) from Kachchh, India: *Journal of Vertebrate Paleontology*, **v. 26**, p. 400–410, https://doi.org/10.1671/0272-4634(2002)022[0861:EPSOTC]2.0.CO;2

Bajpai, S., Thewissen, J.G.M., and Conley, R.W., 2011, Cranial anatomy of middle Eocene Remingtonocetus (Cetacea, Mammalia) from Kutch, India: *Journal of Paleontology*, **v. 85**, p. 703–703.

Banerjee, S., Das, S., Halder, K., and Chakrabarti, N., 2019, Palaeoecological analysis of benthic molluscs from the Eocene of Kutch, Gujarat reveals an event of storm induced concentration of shells in a quiet marginal marine environment: *Journal of the Geological Society of India*, **v. 94**, p. 162–170.

Biswas, S.K., 1992, Tertiary stratigraphy of Kutch: *Journal of the Palaeontological Society of India*, **v. 37**, p. 1–29.

Caldwell, M.W., and Albino, A., 2003, Exceptionally preserved skeletons of the Cretaceous snake *Dinilysia patagonica* Woodward, 1901: *Journal of Vertebrate Paleontology*, **v. 22**, p. 861–866, https://doi.org/10.1671/0272-4634(2002)022[0861:EPSOTC]2.0.CO;2

Calvert, C.J., Mead, A.J., and Parmley, D., 2022, Size estimates of the extinct marine snake *Pterosphenus schucherti* from Eocene-aged sediments of central Georgia: *Georgia Journal of Science*, **v. 80**, article 1, https://digitalcommons.gaacademy.org/gjs/vol80/iss2/1

Catuneanu, O., and Dave, A., 2017, Cenozoic sequence stratigraphy of the Kachchh Basin, India: *Marine and Petroleum Geology*, **v. 86**, p. 1106–1132, https://doi.org/10.1016/j.marpetgeo.2017.07.020

Chatterjee, S., Scotese, C.R., and Bajpai, S., 2017, The restless Indian plate and its epic voyage from Gondwana to Asia: its tectonic, paleoclimatic, and paleobiogeographic evolution: *Geological Society of America Special Paper*, **v. 529**, p. 1–147, https://doi.org/10.1130/SPE529

Cope, E.D., 1868, On new species of extinct reptiles: *Proceedings of the Academy of Natural Sciences of Philadelphia*, **v. 20**, p. 250–266.

Cuvier, G., 1816, Le Règne Animal Distribué d'après son Organisation pour Servir de Base à l'Histoire Naturelle des Animaux et d'Introduction à l'Anatomie Compare: *les Reptiles, les Poissons, les Mollusques et les Annelids*: Paris, Déterville, 532 p.

Cuvier, G., and Valenciennes, A., 1840, Histoire naturelle des poisons, tome quinzième, suite du livre dix-septième: *Siluroïdes*, **v. 15**, p. 1–540.

Datta, D., and Bajpai, S., 2024, Largest known madtsoiid snake from warm Eocene period of India suggests intercontinental Gondwana dispersal: *Scientific Reports*, **v. 14**, n. 8054, https://doi.org/10.1038/s41598-024-58377-0

Datta, D., Mukherjee, D., and Ray, S., 2020, Taphonomic signatures of a new Upper Triassic phytosaur (Diapsida, Archosauria) bonebed from India: aggregation of a juvenile-dominated paleocommunity: *Journal of Vertebrate Paleontology*, **v. 39**, n. e1726361, https://doi.org/10.1080/02724634.2019.1726361

Erickson, B.R., 1998, A palaeophid snake from the late Paleocene of South Carolina: *Transactions of the American Philosophical Society, new ser.*, **v. 88**, no. 4, p. 215–220.

Folie, A., Mees, F., De Putter, T., and Smith, T., 2021, *Presence of the large aquatic snake* Palaeophis africanus *in the middle Eocene marine margin of the Congo Basin*, Cabinda, Angola: Geobios, **v. 66**/67, p. 45–54, https://doi.org/10.1016/j.geobios.2020.11.002

Garberoglio, F.F., Gómez, R.O., and Caldwell, M.W., 2024, New record of aquatic snakes (Squamata, Palaeophiidae) from the Paleocene of South America: *Journal of Vertebrate Paleontology*, **v. 43**, n. e2305892, https://doi.org/10.1080/02724634.2024.2305892

Gayet, M., Rage, J.C., and Rana, R.S., 1984, Nouvelles ichthyofaune et herpétofaune de Gitti Khadan, le plus ancien gisement connu du Deccan (Crétacé/Paléocène) à microvertébrés: implications paléogéographiques, *in* Buffetaut, E., Jaeger, J.J., and Rage, J.C., eds., *Paléogéographie de l'Inde, du Tibet et du Sud-Est Asiatique, Confrontation des Données Paléontologiques avec les Modèles Géodynamiques, Table Ronde, Société Géologique de France et Centre National de la Recherche Scientifique*, Paris, 17–20 October 1983: Paris, La Société Géologique de France, p. 55–65.

Georgalis, G.L., 2023, First potential occurrence of the large aquatic snake *Pterosphenus* (Serpentes, Palaeophiidae) from Nigeria, with further documentation of *Pterosphenus schweinfurthi* from Egypt: Alcheringa: *An Australasian Journal of Palaeontology*, **v. 47**, p. 327–335, https://doi.org/10.1080/03115518.2023.2217874

Georgalis, G.L., and Smith, K.T., 2020, Constrictores Oppel, 1811—the available name for the taxonomic group uniting boas and pythons: *Vertebrate Zoology*, **v. 70**, p. 291–304, https://doi.org/10.26049/VZ70-3-2020-03

Georgalis, G.L., Del Favero, L., and Delfino, M., 2020, Italy's largest snake-redescription of *Palaeophis oweni* (Serpentes, Palaeophiidae) from the Eocene of Monte Duello, near Verona: *Acta Palaeontologica Polonica*, **v. 65**, p. 523–533, https://doi.org/10.4202/app.00711.2019

Georgalis, G.L., Guinot, G., Kassegne, K.E., Amoudji, Y.Z., Johnson, A.K.C., Cappetta, H., and Hautier, L., 2021a, An assemblage of giant aquatic snakes (Serpentes, Palaeophiidae) from the Eocene of Togo: *Swiss Journal of Palaeontology*, **v. 140**, n. 20, https://doi.org/10.1186/s13358-021-00236-w

Georgalis, G.L., Rabi, M., and Smith, K.T., 2021b, Taxonomic revision of the snakes of the genera *Palaeopython* and *Paleryx* (Serpentes, Constrictores) from the Paleogene of Europe: *Swiss Journal of Palaeontology*, **v. 140**, p. 1–140, https://doi.org/10.1186/s13358-021-00224-0

Goloboff, P.A., and Morales, M.E., 2023, TNT version 1.6, with a graphical interface for MacOS and Linux, including new routines in parallel: *Cladistics*, **v. 39**, p. 144–153, https://doi.org/10.1111/cla.12524

Hammer, Ø., and Harper, D.A.T., 2006, *Paleontological Data Analysis*: Malden, Massachusetts, Blackwell 704 Publishing, 351 p.

Head, J.J., Holroyd, P.A., Hutchison, J.H., and Ciochon, R.L., 2005, First report of snakes (Serpentes) from the late middle Eocene Pondaung Formation, Myanmar: *Journal of Vertebrate Paleontology*, **v. 25**, p. 246–250, https://doi.org/10.1671/0272-4634(2005)025[0246:FROSSF]2.0.CO;2

Head, J.J., Howard A.F.C., and Müller, J., 2022, The first 80 million years of snake evolution: the Mesozoic fossil record of snakes and its implications for origin hypotheses, biogeography, and mass extinction, *in* Gower, D., and Zaher, H., eds., *The Origin and Early Evolution of Snakes*: Cambridge, UK, Cambridge University Press, p. 26–54.

Hecht, M.K., Kropach, C., and Hecht, B.M., 1974, Distribution of the yellow-bellied sea snake, *Pelamis platurus*, and its significance in relation to the fossil record: *Herpetologica*, **v. 30**, p. 387–396.

Hoffstetter, R., 1958, Un serpent marin du genre *Pterosphenus* (*Pterosphenus sheppardi* nov. sp.) dans l'Éocène supérieur de l'Equateur (Amérique du Sud): *Bulletin de la Société Geologique de France*, **v. 8**, p. 45–50.

Hoffstetter, R., 1961, Noveaux restes d'un serpent Boidé (*Madtsoia madagascariensis* nov. sp.) dans le Crétacé Supérieur de Madagascar: *Bulletin du Muséum National d'Histoire Naturelle*, sér. 2, **v. 33**, p. 152–160.

Holman, J.A., 1977, Upper Eocene snakes (Reptilia, Serpentes) from Georgia: *Journal of Herpetology*, **v. 11**, p. 141–145.

https://doi.org/10.1017/jpa.2025.10101 Published online by Cambridge University Press

Holman, J.A., 1982, *Palaeophis casei*, new species, a tiny palaeophiid snake from the early Eocene of Mississippi: *Journal of Vertebrate Paleontology*, **v. 2**, p. 163–166.

Houssaye, A., Rage, J.C., Bardet, N., Vincent, P., Amaghzaz, M., and Meslouh, S., 2013, New highlights about the enigmatic marine snake *Palaeophis maghrebianus* (Palaeophiidae; Palaeophiinae) from the Ypresian (lower Eocene) phosphates of Morocco: *Palaeontology*, **v. 56**, p. 647–661, https://doi.org/10.1111/pala.12008

Hutchison, J.H., 1985, *Pterosphenus* cf. *P. schucherti* Lucas (Serpentes, Palaeophidae) from the late Eocene of peninsular Florida: *Journal of Vertebrate Paleontology*, **v. 5**, p. 20–23.

Jain, S.L., and Sahni, A., 1983, Some Upper Cretaceous vertebrates from central India and their paleogeographic implications, *in* Maheshwari, H.K., ed., *Cretaceous of India, Proceedings of the Symposium Cretaceous of India: Palaeoecology, Palaeogeography and Time Boundaries, Lucknow*, November 24−26, 1982: Lucknow, Indian Association of Palynostratigraphers, p. 66–83.

Janensch, W., 1906, Über *Archaeophis proavus* Mass., eine Schlange aus dem Eocän des Monte Bolca: *Beiträge zur Paläontologie und Geologie Österreich-Ungarns und des Orients*, **v. 19**, p. 1–33.

Johnson, R.G., 1955, The adaptive and phylogenetic significance of vertebral form in snakes: *Evolution*, **v. 9**, p. 367–388.

Keller, G., Khozyem, H., Saravanan, N., Adatte, T., Bajpai, S., and Spangenberg, J., 2013, *Biostratigraphy and foraminiferal paleoecology of the early Eocene Naredi Formation, SW Kutch*, India: Geological Society of India Special Publication, **v. 1**, p. 183–196.

Khozyem, H., Adatte, T., Keller, G., Spangenberg, J.E., Saravanan, N., and Bajpai, S., 2013, *Paleoclimate and paleoenvironment of the Naredi Formation (early Eocene)*, Kutch, Gujarat, India: Geological Society of India Special Publication, **v. 1**, p. 165–182.

Kumar, K., and A. Sahni, 1986, *Remingtonocetus harudiensis*, new combination, a middle Eocene archaeocete (Mammalia, Cetacea) from Western Kutch, India: *Journal of Vertebrate Paleontology*, **v. 6**, p. 326–349.

LaDuke, T.C., 1991, Morphometric variability of the precaudal vertebrae of *Thamnophis sirtalis sirtalis* (Serpentes: Colubridae), and implications for interpretation of the fossil record [Ph.D. dissertation]: New York, The City University of New York, 235 p.

LaDuke, T.C., Krause, D.W., Scanlon, J.D. and Kley, N.J., 2010, A Late Cretaceous (Maastrichtian) snake assemblage from the Maevarano Formation, Mahajanga Basin, Madagascar: *Journal of Vertebrate Paleontology*, **v. 30**, p. 109–138, https://doi.org/10.1080/02724630903409188

Linnaeus, C., 1758, *Systema Naturae per Regna Tria Naturae* (tenth edition), Volume **1**, Regnum Animale: Stockholm, Laurentii Salvii, 824 p.

Lucas, F.A., 1898, A new snake from the Eocene of Alabama: *Proceedings of the United States National Museum*, **v. 21**, p. 637, 638.

Lydekker, R., 1888, Notes on Tertiary Lacertilia and Ophidia: *Geological Magazine*, **v. 5**, p. 110–113.

Marsh, O.C., 1892, Notice of new reptiles from the Laramie Formation: *American Journal of Science*, **v. 43**, p. 449–453.

McCartney, J.A., and Seiffert, E.R., 2016, A late Eocene snake fauna from the Fayum Depression, Egypt: *Journal of Vertebrate Paleontology*, **v. 36**, n. e1029580, https://doi.org/10.1080/02724634.2015.1029580

McCartney, J.A., Roberts, E.M., Tapanila, L., and Oleary, M.A., 2018, Large palaeophiid and nigerophiid snakes from Paleogene Trans-Saharan Seaway deposits of Mali: *Acta Palaeontologica Polonica*, **v. 63**, p. 207–220, https://doi.org/10.4202/app.00442.2017

Mohabey, D.M., Head, J.J., and Wilson Mantilla, J.A., 2011, A new species of the snake *Madtsoia* from the Upper Cretaceous of India and its paleobiogeographic implications: *Journal of Vertebrate Paleontology*, **v. 31**, p. 588–595, https://doi.org/10.1080/02724634.2011.560220

Mosauer, W., 1932, On the locomotion of snakes: *Science*, **v. 76**, p. 583–585.

Müller, J., and Henle, F.G.J., 1837, Gattungen der Haifische und Rochen nach einer von ihm mit Herrn Henle unternommenen gemeinschaftlichen Arbeit über die Naturgeschichte der Knorpelfische: *Berichte der Königlichen Preußischen Akademie der Wissenschaften zu Berlin*, **v. 2**, p. 111–118.

Mukherjee, D., and Ray, S., 2012, Taphonomy of an upper Triassic vertebrate bonebed: a new rhynchosaur (Reptilia; Archosauromorpha) accumulation from India: *Palaeogeography, Palaeoclimatology, Palaeoecology*, **v. 333**, p. 75–91, https://doi.org/10.1016/j.palaeo.2012.03.010

Mukhopadhyay, S., and Shome, S., 1996, Depositional environment and basin development during early Palaeogene lignite deposition, western Kutch, Gujarat: *Journal of the Geological Society of India*, **v. 47**, p. 579–592.

Natarajan, A., Dasgupta, S., Rakshit, N., and Kashyap, Y., 2024, Taxonomic revision of the giant marine snake genus *Pterosphenus* Lucas, 1898, based on new fossil material from the middle Eocene (Bartonian) Harudi Formation of Kachchh (Kutch) Basin, India: *Journal of Vertebrate Paleontology*, **v. 43**, n. e2375332, https://doi.org/10.1080/02724634.2024.2375332

Oppel, M., 1811, *Die Ordnungen, Familien und Gattungen der Reptilien als Prodrom einer Naturgeschichte derselben: Munich*, Joseph Lindauer, 87 p.

Owen, R., 1841, Description of some ophidiolites (*Palæophis toliapicus*) from the London Clay of Sheppey, indicating an extinct species of serpent: *Transactions of the Geological Society ser.* **2**, v. 6, p. 209–210.

Owen, R., 1850, Ophidia (*Palæophis*, &c.), *in* Owen, R., ed., *Monograph on the Fossil Reptilia of the London Clay and of the Bracklesham and Other Tertiary Beds*: London, Palæontographical Society of London, p. 51–63.

Parmley, D., and Case, G.R., 1988, Palaeopheid snakes from the Gulf coastal region of North America: *Journal of Vertebrate Paleontology*, **v. 8**, p. 334–339.

Parmley, D., and DeVore, M., 2005, Palaeophid snakes from the late Eocene Hardie Mine local fauna of central Georgia: *Southeastern Naturalist*, **v. 4**, p. 703–722, https://doi.org/10.1656/1528-7092(2005)004[0703:PSFTLE]2.0.CO;2

Parmley, D., and Reed, H.W., 2003, Size and age class estimates of North American Eocene palaeopheid snakes: *Georgia Journal of Science*, **v. 61**, p. 220–232.

Prasad, G.V.R., and Khajuria, C.K, 1996, Palaeoenvironment of the Late Cretaceous mammal-bearing intertrappean beds of Naskal, Andhra Pradesh, India: *Memoirs of the Geological Society of India*, **v. 37**, p. 337–362.

Prasad, G.V.R., and Rage, J.-C., 1995, Amphibians and squamates from the Maastrichtian of Naskal (India): *Cretaceous Research*, **v. 16**, p. 95–107.

Prasad, G.V.R., and Sahni, A., 1987, Coastal-plain microvertebrate assemblage from the terminal Cretaceous of Asifabad, peninsular India: *Journal of the Palaeontological Society of India*, **v. 32**, p. 5–19.

Pritchard, A.C., McCartney, J.A., Krause, D.W., and Kley, N.J., 2014, New snakes from the Upper Cretaceous (Maastrichtian) Maevarano Formation, Mahajanga Basin, Madagascar: *Journal of Vertebrate Paleontology*, **v. 34**, p. 1080–1093, https://doi.org/10.1080/02724634.2014.841706

Pyron, R.A., Reynolds, R.G., and Burbrink, F.T., 2014, A taxonomic revision of boas (Serpentes: Boidae): *Zootaxa*, **v. 3846**, p. 249–260, https://doi.org/10.11646/zootaxa.3846.2.5

Rage, J.-C., 1975, Un serpent du Paléocène du Niger: étude préliminaire sur l'origine des Caenophidiens (Reptilia, Serpentes): *Comptes Rendus de l'Académie des Sciences de Paris*, **v. 281**, p. 515–518.

Rage, J.-C., 1983a, *Palaeophis colossaeus* nov. sp. (le plus grand serpent connu?) de l'Éocène du Mali et le problème du genre chez les Palaeopheinae: *Comptes Rendus des Séances de l'Académie des Sciences de Paris*, **v. 296**, p. 1029–1032.

Rage, J.-C., 1983b, Les serpents aquatiques de l'Éocène Européen: définition des espèceset aspects stratigraphiques: *Bulletin du Muséum National d'Histoire Naturelle, sér. 4, section C, Sciences de la Terre, Paléontologie, Géologie, Minéralogie*, **v. 5**, p. 213–241.

Rage, J.-C., 1984, *Handbuch der Paläoherpetologie, Teil 11*, Serpentes: Stuttgart, Gustav Fischer Verlag, 80 p.

Rage, J.-C., and Prasad, G.V.R., 1992, New snakes from the Late Cretaceous (Maastrichtian) of Naskal, India: *Neues Jahrbuch für Geologie und Paläontologie, Abhandlungen*, **v. 187**, p. 83–97.

Rage, J.-C., and Wouters, G., 1979, Découverte du plus ancien palaeopheidé (Reptilia, Serpentes) dans le Maestrichtien du Maroc: *Geobios*, **v. 12**, p. 293–296.

Rage, J.-C., Bajpai, S., Thewissen, J.G., and Tiwari, B.N., 2003, Early Eocene snakes from Kutch, western India, with a review of the Palaeophiidae: *Geodiversitas*, **v. 25**, p. 695–716.

Rage, J.-C., Prasad, G.V.R., and Bajpai, S., 2004, Additional snakes from the uppermost Cretaceous (Maastrichtian) of India: *Cretaceous Research*, **v. 25**, p. 425–434, https://doi.org/10.1016/j.cretres.2004.02.003

Rage, J.-C., Folie, A., Rana, R.S., Singh, H., Rose, K.D., and Smith, T., 2008, *A diverse snake fauna from the early Eocene of Vastan Lignite Mine*, Gujarat, India: Acta Palaeontologica Polonica, **v. 53**, p. 391–403, https://doi.org/10.4202/app.2008.0303

Rage, J.C., Vullo, R., and Neraudeau, D., 2016, The mid-Cretaceous snake *Simoliophis rochebrunei* Sauvage, 1880 (Squamata: Ophidia) from its type

https://doi.org/10.1017/jpa.2025.10101 Published online by Cambridge University Press

area (Charentes, southwestern France): redescription, distribution, and palaeoecology: *Cretaceous Research*, **v. 58**, p. 234–253, https://doi.org/10.1016/j.cretres.2015.10.010

Rage, J.-C., Prasad, G.V.R., Verma, O., Khosla, A., and Parmar, V., 2020, Anuran Lissamphibian and squamate reptiles from the Upper Cretaceous (Maastrichtian) Deccan Intertrappean Sites in Central India, with a review of Lissamphibian and squamate diversity in the northward drifting Indian plate, *in* Prasad, G.V.R., and Patnaik, R., eds., *Biological Consequences of Plate Tectonics: New Perspectives on Ppost-Gondwana Break-up*: Cham, Switzerland, Springer Nature Switzerland, p. 99–121.

Ravikant, V., and Bajpai, S., 2010, Strontium isotope evidence for the age of Eocene fossil whales of Kutch, western India: *Geological Magazine*, **v. 147**, p. 473–477, https://doi.org/10.1017/S0016756810000099

Rio, J.P., and Mannion, P.D., 2017, The osteology of the giant snake *Gigantophis garstini* from the upper Eocene of North Africa and its bearing on the phylogenetic relationships and biogeography of Madtsoiidae: *Journal of Vertebrate Paleontology*, **v. 37**, n. e1347179, https://doi.org/10.1080/02724634.2017.1347179

Sahni. A., and Mishra, V.P., 1975. Lower Tertiary vertebrates from western India: *Monograph of the Palaeontological Society of India*, **v. 3**, p. 1–48.

Sauvage, H.E., 1880, Sur l'existence d'un reptile du type ophidien dans les couches à *Ostrea columba* des Charentes: *Comptes Rendus Hebdomadaires des Séances de l'Académie des Sciences*, v. **91**, p. 671, 672.

Scanferla, C.A., and Canale, J.I., 2007, The youngest record of the Cretaceous snake genus *Dinilysia* (Squamata, Serpentes): *South American Journal of Herpetology*, **v. 2**, p. 76–81, https://doi.org/10.2994/1808-9798(2007)2[76:TYROTC]2.0.CO;2

Serra-Kiel, J., Hottinger, L., Caus, E., Drobne, K., Ferrandez, C., et al., 1998, Larger foraminiferal biostratigraphy of the Tethyan Paleocene and Eocene: *Bulletin de la Société Géologique de France*, **v. 169**, p. 281–299.

Smith, K.T., and Georgalis, G.L., 2022, The diversity and distribution of Palaeogene snakes: a review with comments on vertebral sufficiency, *in* Gower, D., and Zaher, H., eds., *The Origin and Early Evolution of Snakes*: Cambridge, UK, Cambridge University Press, p. 55–84.

Smith, T., Kumar, K., Rana, R.S., Folie, A., Solé, F., Noiret, C., Steeman, T., Sahni, A. and Rose, K.D., 2016, New early Eocene vertebrate assemblage from western India reveals a mixed fauna of European and Gondwana affinities: *Geoscience Frontiers*, **v. 7**, p. 969–1001, https://doi.org/10.1016/j.gsf.2016.05.001

Smith-Woodward, A., 1901, On some extinct reptiles from Patagonia of the genera *Miolania*, *Dinilysia*, and *Genyodectes*: *Proceedings of the Zoological Society of London*, **v. 70**, p. 169–184.

Snetkov, P.B., 2011, Vertebrae of the sea snake *Palaeophis nessovi* Averianov (Acrochordoidea, Palaeophiidae) from the Eocene of western Kazakhstan and phylogenetic analysis of the superfamily Acrochordoidea: *Paleontological Journal*, **v. 45**, p. 305–313, https://doi.org/10.1134/S0031030111030129

Szyndlar, Z., and Georgalis, G.L., 2023, An illustrated atlas of the vertebral morphology of extant non-caenophidian snakes, with special emphasis on the cloacal and caudal portions of the column: *Vertebrate Zoology*, **v. 73**, p. 717–886, https://doi.org/10.3897/vz.73.e101372

Tatarinov, L.P., 1963, First occurrence of ancient sea snakes in the USSR: *Paleontologičeskij Žurnal*, **v. 2**, p. 109–115.

Thewissen, J.G. and Bajpai, S., 2009, New skeletal material of *Andrewsiphius* and *Kutchicetus*, two Eocene cetaceans from India: *Journal of Paleontology*, **v. 83**, p. 635–663, https://doi.org/10.1666/08-045.1

Thewissen, J.G.M., Cooper, L.N., George, J.C., and Bajpai, S., 2009, From land to water: the origin of whales, dolphins, and porpoises: Evolution: *Education and Outreach*, **v. 2**, p. 272–288, https://doi.org/10.1007/s12052-009-0135-2

Wazir, W.A., Sehgal, R.K., Čerňanský, A., Patnaik, R., Kumar, N., Singh, A. P., Uniyal, P., and Singh, N.P., 2021, A find from the Ladakh Himalaya reveals a survival of madtsoiid snakes (Serpentes, Madtsoiidae) in India through the late Oligocene: *Journal of Vertebrate Paleontology*, **v. 41**, n. e2058401, https://doi.org/10.1080/02724634.2021.2058401

Westgate, J.W., 2001, Paleoecology and biostratigraphy of marginal marine Gulf Coast Eocene vertebrate localities, *in* Gunnel, G.F., ed., *Eocene Biodiversity: Unusual Occurrences and Rarely Sampled Habitats*: New York, Kluwer Academic/Plenum, p. 263–297.

Westgate, J.W., and Gee, C.T., 1990, Paleoecology of a middle Eocene mangrove biota (vertebrates, plants, and invertebrates) from southwest Texas: *Palaeogeography, Palaeoclimatology, Palaeoecology*, **v. 78**, p. 163–177.

Westgate, J.W., and Ward, J.F., 1981, The giant aquatic snake *Pterosphenus schucherti* (Palaeophidae) in Arkansas and Mississipi: *Journal of Vertebrate Paleontology*, **v. 1**, p. 161–164.

Wilson Mantilla, J.A., Mohabey, D.M., Peters, S.E., and Head, J.J., 2010, Predation upon hatchling dinosaurs by a new snake from the Late Cretaceous of India: *PLoS Biology*, **v. 8**, n. e1000322, https://doi.org/10.1371/journal.pbio.1000322

Zaher, H., Folie, A., Quadros, A.B., Rana, R.S., Kumar, K., Rose, K.D., Fahmy, M., and Smith, T., 2021, Additional vertebral material of *Thaumastophis* (Serpentes: Caenophidia) from the early Eocene of India provides new insights on the early diversification of colubroidean snakes: *Geobios*, **v. 66**, p. 35–43, https://doi.org/10.1016/j.geobios.2020.06.009

Zaher, H., Mohabey, D.M., Grazziotin, F.G., and Wilson Mantilla, J.A., 2023, The skull of *Sanajeh indicus*, a Cretaceous snake with an upper temporal bar, and the origin of ophidian wide-gaped feeding: *Zoological Journal of the Linnean Society*, **v. 197**, p. 656–697, https://doi.org/10.1093/zoolinnean/zlac001

Zigno, A. de, 1881, Nuove aggiunte alla fauna eocena del Veneto: *Memorie del Reale Istituto Veneto di Scienze, Lettere ed Arti*, **v. 21**, p. 775–790.

Zouhri, S., Khalloufi, B., Bourdon, E., de Broin, F.D.L., Rage, J.-C., M'haïdrat, L., Gingerich, P.D., and Elboudali, N., 2018, Marine vertebrate fauna from the late Eocene Samlat Formation of Ad-Dakhla, southwestern Morocco: *Geological Magazine*, **v. 155**, p. 1596–1620, https://doi.org/10.1017/S0016756817000759

Zouhri, S., Gingerich, P.D., Khalloufi, B., Bourdon, E., Adnet, S., et al., 2021, Middle Eocene vertebrate fauna from the Aridal Formation, *Sabkha of Gueran, southwestern Morocco: Geodiversitas*, **v. 43**, p. 121–150, https://doi.org/10.5252/geodiversitas2021v43a5

Zvonok, E.A., and Snetkov, P.B., 2012, New findings of snakes of the genus *Palaeophis* Owen, 1841 (Acrochordoidea: Palaeophiidae) from the middle Eocene of Crimea: *Proceedings of the Zoological Institute RAS*, **v. 316**, p. 392–400, https://doi.org/10.31610/trudyzin/2012.316.4.392

Appendix 1. Holotype and referred specimens examined. All specimens are partial or nearly complete, if not mentioned otherwise

Registration no.	Material	Registration no.	Material
Vertebrae of *Pterosphenus rannensis* n. sp. (N = 12)		Vertebra of ?*Palaeophis* sp. indet. (N = 1)	
IITR/VPL/SB 3014–1	Anterior trunk vertebra	IITR/VPL/SB 2632	Middle trunk vertebra
IITR/VPL/SB 3014–2	?Middle trunk vertebra	Vertebra of Madtsoiidae gen. indet. sp. indet. (N = 1)	
IITR/VPL/SB 3014–3	Anterior trunk vertebra	IITR/VPL/SB 2782	Middle trunk vertebra
IITR/VPL/SB 3014–4	Precloacal vertebra	Vertebra of ?Nigerophiidae gen. indet. sp. indet. (N = 1)	
IITR/VPL/SB 3014–5	Middle trunk vertebra	IITR/VPL/SB 97	Precloacal vertebra
IITR/VPL/SB 3014–6	Middle trunk vertebra		
IITR/VPL/SB 3014–7	Middle trunk vertebra		
IITR/VPL/SB 3014–8	Precloacal vertebra		
IITR/VPL/SB 3014–9	Precloacal vertebra		
IITR/VPL/SB 3014–10	Precloacal vertebra		
IITR/VPL/SB 3015	Anterior trunk vertebra		
IITR/VPL/SB 2980	Middle trunk vertebra		

https://doi.org/10.1017/jpa.2025.10101 Published online by Cambridge University Press

Appendix 2. Measurement of vertebral specimens (IITR/VPL/SB). All measurements in mm unless otherwise indicated. b. = measurement of broken regions; β = angle (when added to anatomical abbreviations); H = height; L = length; W = width. CL = centrum length; CNH = condyle height; CNW = condyle width; COH, cotyle height; COW, cotyle width; NAW, neural arch width; NCH, neural canal; NCW, neural canal width; NSH, neural spine height; POFL = postzygapophyseal facet length; POFW = postzygapophyseal facet width; POW = postzygapophyseal width; POα = postzygapohyseal angle; PRFL = prezygapophyseal facet length; PRFW = prezygapophyseal facet width; PRW = prezygapophyseal width; PRα = prezygapophyseal angle; TVH = total vertebral height; ZSFL = zygosphenal facet length; ZSFW = zygosphenal facet width; ZSH = zygosphene height; ZSW = zygosphene width; ZSβ = zygosphene angle

Registration no.	CL	COH	COW	CNH	CNW	SYW	NCH	NCW	NAW	NSH	NSL	POFL
3014–1	26.1	15.6	17.5	13.1	15.3	~24.3	4.7	7.5	21.6	20.6	13.9	7.9
3014–2	24.8	14.5	17	13.8	b.13.6	~17.7	21.4	4.8	21.7	-	-	7.6
3014–3	21.9	14.8	13.9	13.6	13.9	-	5.6	8.9	19.3	-	13.3	5.8
3014–4	-	-	-	-	-	-	~5.8	9.9		14.6	14.8	6.9
3014–5	21	12.9	14.9	11.7	13.8	21.4	4.7	9.4	21.22	-	11.1	6
3014–6	20.8	12.4	14.7	12.5	14.2	22.8	4.7	7.7	22.5	-	-	-
3014–7	20.9	12.5	14.3	12.7	14.6	-	4.1	7.7	21.7	-	10.7	4.2
3014–8	20.2	11.5	12.9	10.2	12.2	-	4.6	8.8	21.2	-	-	-
3014–9	20.5	12.5	b.7.4	-	11.9	-	4.7	7.9	-	-	-	-
3014–10	23.6	-	16.1	13.2	14.9	-	5.9	7.8	21.4	-	-	-
3015	22.2	13.8	16.6	12.1	11.1	20.5	-	-	-	-	-	-
2980	17.3	13.6	14.6	9.7	10.3	-	5.1	7.1	b.17.9	-	-	-
2632	28	15.9	17.9	14.5	16.4	23.5	6.4	9.2	23.5	-	11.9	6.5
2782	67.9	35.4	42.1	35.3	40.4	110.1	12.3	37.9	76.3	8.6	15.7	24.8
97	10.16	4.9	5.5	4	4.1	4.3	2.6	4.7	8.4	0.8	3.7	2.7

Registration no.	POFW	POW	POα	PRFL	PRFW	PRW	PRα	TVH	ZSFL	ZSFW	ZSH	ZSW	ZSβ
3014–1	5.5	20.8	6°	8.4	5.6	25.1	25°	52.8	7.6	5.8	9.3	~14.7	115°
3014–2	6.8	~25	3°	8.4	5.8	~24	6°	-	7.4	5.8	9.7	~13.1	118°
3014–3	6.2	~25	-	6.2	4.5	~22		-	6.4	6.3	-	b.18	120°
3014–4	6	25.5	-	-	-	-	-	-	5	5.2	9.4	15.9	114°
3014–5	5.2	~25	14°	7.3	4.8	23.1	9°	-	6.7	4.8	11.3	14.9	125°
3014–6	-	-	-	7.4	5.2	23.5	8°	-	6.9	4.4	9.7	14.7	122°
3014–7	3.3	~21	16°	6.3	5.9	~22	17°	-	6.7	5.5	10.7	15.1	120°
3014–8	-	-	-	6.8	6	~21	9°	-	5	5.6	7.7	13.5	130°
3014–9	-	-	-	6.5	5.2	~22	25°	-	5.4	5	7.3	14.4	109°
3014–10	-	-	-	8.8	4.9	~21	15°	-	6.3	5.1	8.4	15	109°
3015	-	-	-	-	-	-	-	-	-	-	-	-	-
2980	-	-	-	-	-	-	-	-	4.7	5.6	9	13.8	143°
2632	4.4	~27		8.6	~4.9	~24		-	-	-	-	-	-
2782	21.8	93.9	31°	28.2	22.6	95.8	35°	95.4	25.2	26.4	25.1	b.39	92°
97	2.4	~9.8	-	3.4	1.4	~11	5°	13.5	2.8	1.7	2.5	~5.1	143°

https://doi.org/10.1017/jpa.2025.10101 Published online by Cambridge University Press

Appendix 3. Characters used in the phylogenetic analysis. A brief explanation follows the new characters used, whereas for a character already used in previous literature, its citation follows the last character state. S = Snetkov (2011). Numerals indicate the character number of each citation

1. Shape of the zygosphene: dorsal surface devoid of dorsoventrally high central crest (0); dorsal surface bearing dorsoventrally high central crest (1) [modified after S1]. The character was modified to adequately cover the difference/variation in shape of the zygosphene between *Palaeophis* and *Pterosphenus*-grade snakes.
2. Thickness of the zygosphene: thin (width more than twice as great as the thickness) (0); thick (width is less than twice as great as the thickness) (1) [S2].
3. Presence of the anterior hypapophysis on the anterior trunk vertebrae: vertebrae in the anterior part of the vertebral column lack anterior hypapophyses, which are much more developed than hypapophysis on other trunk vertebrae (0); vertebrae in the anterior part of the vertebral column have anterior hypapophyses, which are much more developed than that of other trunk vertebrae (1) [S3].
4. Presence of the anterior hypapophysis on the vertebrae of the middle and posterior trunk region: absent (0); present (1) [S4].
5. Relative height of the neural canal in the middle trunk vertebrae in anterior view: height ratio of the neural canal and cotyle > 0.4 (0); ratio < 0.4 (1) [S5].
6. Presence of the interzygapophyseal ridge: absent or very weak (0); well developed (1) [S6].
7. Shape of the centrum: condyle positioned much lower than cotyle (0); condyle positioned at the same level as cotyle (1) [S8].
8. Size of the prezygapophyses: large (ratio of prezygapophysis length to height of the cotyle > 0.7) (0); small (ratio < 0.7) (1) [S10].
9. Position of the prezygapophyses: medial part of the articular surface of the prezygapophyses positioned above the dorsal surface of the centrum (0); medial part of the articular surface of the prezygapophyses positioned at the level of the dorsal surface of the centrum (1) [S11].
10. Shape of the prezygapophyses: articular surfaces strongly inclined (0); articular surfaces positioned almost horizontally (1) [S12].
11. Position of synapophyses on middle trunk vertebrae: dorsal to ventral cotylar rim (0); extending slightly for a short distance below ventral cotylar rim (1); extending strongly below ventral cotylar rim (2) [modified after S13]. Modifications were introduced to adequately cover the variation in morphology seen in the examined taxa.
12. Extent of lateral flattening of the middle trunk vertebrae: slightly flattened prW/cL ≥ 1 (0); strongly flattened prW/cL < 1 (1) [modified after S14]. Modifications were made to evaluate the lateral flattening of the vertebrae in a quantitative manner.
13. Length of the centrum in the vertebrae that do not belong to the posterior trunk region in ventral view: less than the distance between the lateral margins of the synapophyses (0); more than the distance between the lateral margins of the synapophyses (1) [S15].
14. Position of the neural spine: anterior margin not extending to the dorsal margin of the zygosphene (0); anterior margin extending to the dorsal margin of the zygosphene (1) [modified after S16]. The character was modified to adequately cover the variation in neural spine morphology seen in palaeophiine snakes.
15. Presence of subcentral foramina: absent (0); present (1) [S17].
16. Development of the haemal keel on the middle trunk vertebrae: well developed, gradually passing into the posterior hypapophysis, which projects slightly more strongly than the haemal keel (0); poorly developed, projecting to a considerably lesser extent than the posterior hypapophysis (1) [S18].
17. Shape of the condyle: inclined strongly anteriorly (0); almost lacking anterior inclination (1) [S19].
18. Shape of the cross section of the centrum: ovate (0); almost triangular (1) [S20].
19. Width of the neural canal in the middle part of the vertebra: not wider than the centrum (0); much wider than the centrum (1) [S21].
20. Presence of subcentral crests on the anterior and middle trunk vertebrae: present (0); absent (1) [S22].
21. Width of the zygosphene: wide (width more than half the distance between the lateral ends of the prezygapophyses) (0); narrow (width less than half of the distance between the lateral ends of the prezygapophyses) (1) [S23].
22. Height of the vertebra: distance between the lateral margins of prezygapophyses more than the vertebral height from the ventral side of the cotyle to the dorsal margin of the zygosphene (0); distance between the lateral margins of prezygapophyses less than the vertebral height from the ventral side of the cotyle to the dorsal margin of the zygosphene (1) [S24].
23. Height of the neural arch: ratio of the distance from the dorsal side of the centrum to the dorsal margin of the zygosphene to the distance between the lateral margins of prezygapophyses < 0.4 (0); ratio > 0.4 (1) [S25].
24. Shape of the neural canal in anterior view: lateral margins strongly inclined (0); lateral margins almost vertical (1) [S26].
25. Angle formed by the margins of the V-shaped incisure in the posterior part of the neural arch in the vertebrae that do not belong to the posterior trunk region: > 105° (0); < 105° (1) [S27].
26. Shape of the posterior part of the neural arch in posterior view: distance from the dorsal surface of the centrum to the dorsal margin of the zygantrum greater than the distance from the dorsal margin of the zygantrum to the bases of pterapophyses (0); distance from the dorsal surface of the centrum to the dorsal margin of the zygantrum less than the distance from the dorsal margin of the zygantrum to the bases of pterapophyses (1) [S28].
27. Prezygapophyseal buttress: buttress lacking convexity or weakly convex (0); buttress strongly convex (1). In basal forms, e.g., *Dinillysia* Smith-Woodward, 1901, the prezygapophyseal buttress lacks convexity (coded as 0). In most palaeophiines the buttress bears a convexity (coded as 1).
28. Pterapophysis in precloacal vertebrae: absent (0); present but remaining below or at par with the dorsal zygosphenal margin (1); present and extending slightly above the dorsal zygosphenal margin (2); present and extending well above the dorsal zygosphenal margin (3). In basal forms such as *Dinilysia*, a pterapophysis is absent (coded as 0). Within Palaeophiinae, in *Palaeophis* snakes, the pterapophysis extends slightly above the zygosphene (coded as 2). In most *Pterosphenus* snakes, the pterapophysis extends well above the zygophene (coded as 3). The pterapophysis remains below the zygosphene in *Pterosphenus rannensis* n. sp. (coded as 1).
29. Height of pterapophysis (PTH) relative to centrum length (CL): PTH/CL ≤ 0.4 (0); 0.4 < PTH/CL ≤ 0.7 (1); PTH/CL > 0.7 (2). In 'primitive'-grade palaeophiids (e.g., *Palaeophis maghrebianus* and *Palaeophis africanus*), PTH/CL is ≤ 0.4 (coded as 0), whereas in 'advanced'-grade palaeophiids (e.g., *Palaeophis toliapicus* and *Palaeophis typhaeus*), PTH/CL ranges between 0.4 and 0.7 (coded as 1). In *Pterosphenus* taxa (e.g., *Pterosphenus schucherti* and *Pterosphenus schweinfurthi*), PTH/CL is > 0.7 (coded as 2).
30. Pterapophysis-postzygapophysis connection in lateral view: straight/weakly concave (0); markedly concave (1). In *Palaeophis* snakes (e.g., *Palaeophis maghrebianus* and *Palaeophis typhaeus*), the pterapophysis-postzygapophysis connection is weakly concave or devoid of it (coded as 0), whereas in most *Pterosphenus* taxa, the pterapophysis-postzygapophysis connection is markedly concave (coded as 1).

https://doi.org/10.1017/jpa.2025.10101 Published online by Cambridge University Press